PB85-216653

Selenium Removal from Drinking Water by Ion Exchange

California Univ., Richmond

Prepared for

Environmental Protection Agency, Cincinnati, OH

Jun 85

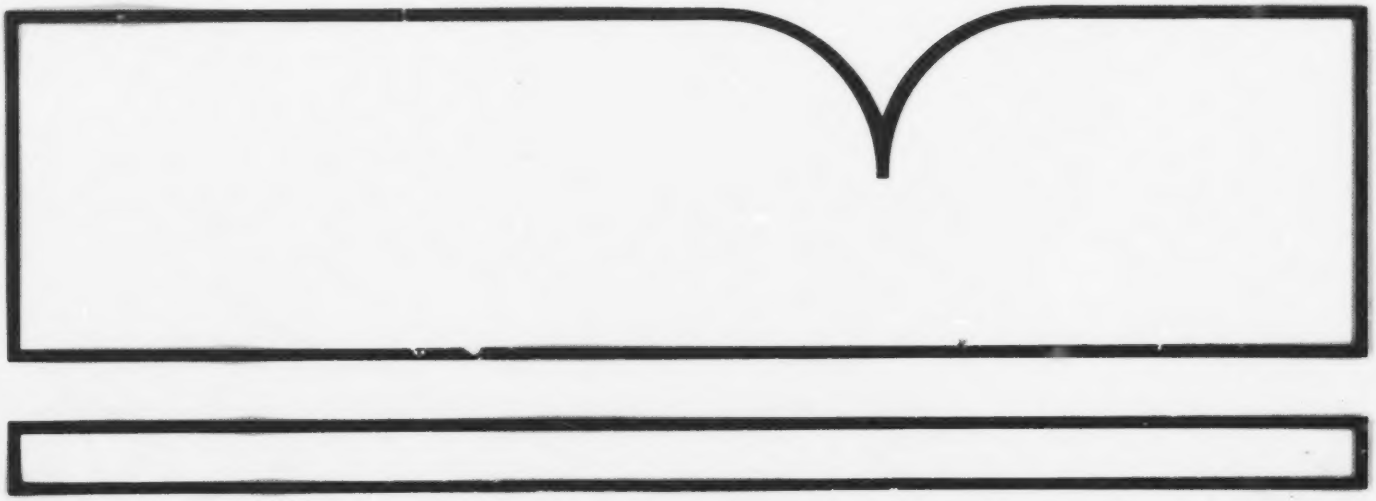

U.S. Department of Commerce
National Technical Information Service
NTIS

PB85-216653

EPA/600/2-85/074
June 1985

SELENIUM REMOVAL FROM DRINKING WATER BY ION EXCHANGE

BY

James E. Maneval, Gerhard Klein and Jelena Sinkovic
Water Thermal and Chemical Technology Center
Richmond, California 94804

Cooperative Agreement CR-810254

Project Officer

Richard P. Lauch
Drinking Water Research Division
Water Engineering Research Laboratory
Cincinnati, Ohio 45268

REPRODUCED BY
NATIONAL TECHNICAL
INFORMATION SERVICE
U.S. DEPARTMENT OF COMMERCE
SPRINGFIELD, VA. 22161

WATER ENGINEERING RESEARCH LABORATORY
OFFICE OF RESEARCH AND DEVELOPMENT
U.S. ENVIRONMENTAL PROTECTION AGENCY
CINCINNATI, OHIO 45268

TECHNICAL REPORT DATA
(Please read Instructions on the reverse before completing)

1. REPORT NO. EPA/600/2-85/074	2.
3. RECIPIENT'S ACCESSION NO. PB85 216653/AS	
4. TITLE AND SUBTITLE Selenium Removal from Drinking Water by Ion Exchange	5. REPORT DATE June 1985
	6. PERFORMING ORGANIZATION CODE
7. AUTHOR(S) James E. Maneval, Gerhard Klein & Jelena Sinkovic	8. PERFORMING ORGANIZATION REPORT NO.
9. PERFORMING ORGANIZATION NAME AND ADDRESS Water Thermal & Chemical Technology Center Richmond, California 94804	10. PROGRAM ELEMENT NO.
	11. CONTRACT/GRANT NO. CR810254
12. SPONSORING AGENCY NAME AND ADDRESS Water Engineering Research Laboratory -- Cin.,OH Office of Research & Development U.S. Environmental Protection Agency Cincinnati, OH 45268	13. TYPE OF REPORT AND PERIOD COVERED Project 9/82 to 9/84
	14. SPONSORING AGENCY CODE EPA/600/14

15. SUPPLEMENTARY NOTES

Project Officer: Richard P. Lauch 513/684-7467

16. ABSTRACT

Strong-base anion exchangers were shown to remove selenate and selenite ions from drinking water. Because selenium species are usually present at low concentrations, the efficiency of removal is controlled by the concentration of the common drinking water anions, the most important being sulfate. The ion-exchange behavior of selenate was found to be identical to that of sulfate, while the behavior of selenite was found to be similar to that of nitrate. The local-equilibrium theory for ion-exchange columns produced good results in predicting selenium removal capacities.

Two alternative methods of selenium removal were also investigated. Attempts to find reagents, compatible with water treatment, that were capable of reducing selenate to selenite (for which there are selective removal methods) were unsuccessful. Screening experiments showed that a weak-acid cation exchanger in the ferric form selectively removed selenite from water containing the common drinking-water anions.

17. KEY WORDS AND DOCUMENT ANALYSIS

a. DESCRIPTORS	b. IDENTIFIERS/OPEN ENDED TERMS	c. COSATI Field/Group
Potable Water Selenium Removal Ion Exchange		

18. DISTRIBUTION STATEMENT Release to Public	19. SECURITY CLASS *(This Report)* Unclassified	21. NO. OF PAGES 73
	20. SECURITY CLASS *(This page)* Unclassified	22. PRICE

EPA Form 2220-1 (Rev. 4-77) PREVIOUS EDITION IS OBSOLETE

DISCLAIMER

The information in this document has been funded wholly or in part by the United States Environmental Protection Agency under Cooperative Agreement No. 810254 to the Water Thermal and Chemical Technology Center. It has been subject to the Agency's peer and administrative review, and has been approved for publication as as EPA document. Mention of trade names or commercial products does not constitute endorsement or recommendation for use.

FOREWORD

The U. S. Environmental Protection Agency is charged by Congress with protecting the Nation's land, air and water systems. Under a mandate of national environmental laws, the agency strives to formulate and implement actions leading to a compatible balance between human activities and the ability of natural systems to support and nuture life. The Clean Water Act, the Safe Drinking Water Act, and the Toxic Substances Control Act are three of the major congressional laws that provide the framework for resoring and maintaining the integrity of our Nation's water, for preserving and enhancing the water we drink, and for protecting the environment from toxic substances. These laws direct the EPA to perform research to define our environmental problems, measure the impacts and search for solutions.

The Water Engineering Research Laboratory is that component of EPA's Research and Development program concerned with preventing, treating and managing municipal and industrial wastewater dicharges; establishing practices to control and remove contaminants from drinking water and to prevent its deterioration during storage and distribution; and assessing the nature and controllability of release of toxic substances to the air, water and land from manufacturing processes and subsequent product uses. This publication is one of the products of that research and provides a vital communication link between the research and the user community.

The present study is concerned with the applicability of ion exchange to the removal of selenium from drinking water.

Francis T. Mayo, Director Water Engineering
Research Laboratory

ABSTRACT

Strong-base anion exchangers were shown to remove selenate and selenite ions from drinking water. Because selenium species are usually present at low concentrations, the efficiency of removal is controlled by the concentration of the common drinking water anions, the most important being sulfate. The ion-exchange behavior of selenate was found to be identical to that of sulfate, while the behavior of selenite was found to be similar to that of nitrate. The local-equilibrium theory for ion-exchange columns produced good results in predicting selenium removal capacities.

Two alternative methods of selenium removal were also investigated. Attempts to find reagents, compatible with water treatment, that were capable of reducing selenate to selenite (for which there are selective removal methods) were unsuccessful. Screening experiments showed that a weak-acid cation exchanger in the ferric form selectively removed selenite from water containing the common drinking-water anions.

This report was submitted in fulfillment of Cooperative Agreement number CR-810254 by the Water Thermal and Chemical Technology center under the partial sponsorship of the U. S. Environmental Protection Agency. This report covers a period from September, 1982 to July, 1984 and the work was completed as of July, 1984.

CONTENTS

Disclaimer ii
Foreword iii
Abstract iv
Figures vi
Tables vii
Acknowledgments viii
List of Symbols ix

1. Introduction 1
2. Conclusions and Recommendations 2
3. Background Information 3
    Chemical Aspects 3
    Basic Concepts For Fixed-Bed Analysis 5
        Equilibrium Behavior and Models 5
        Column Behavior 11
4. Selenium Removal Study 13
    Ion Exchange Equilibria Involving Selenium 13
    Utilization of Equilibrium Data for Performance Prediction 19
    Column Studies 24
        Exhaustion Runs 24
        Regeneration Runs 24
    Novel Removal Techniques 26
5. Design Example 30

Appendix A1. Equilibrium and Fixed-Bed Theory 32
    1. Constant-Separation-Factor Model 32
    2. Effluent Concentration Histories and Concentration Profiles 33
    3. Prediction of Fixed-Bed Performance 35
        3.1 Binary Systems 35
        3.2 Ternary Systems 35
        3.3 Higher-Order Systems 39
    4. Trace Behavior 39
Appendix A2. Discussion of Figures 9 and 10 40
Appendix A3. Discussion of Figure 11 42
Appendix A4. Experimental Methods for Generating Isotherms 46
    1. Batch Method 46
    2. Column Method 46
Appendix A5. Column Experiments 52
Appendix A6. Analytical Methods 58

References 59

FIGURES

Figure 1. Three-component effluent concentration history.. 6
Figure 2. Constant-separation-factor model isotherms..... 8
Figure 3. Mass-action model isotherms..... 10
Figure 4. Three-component effluent concentration history.. 12
Figure 5. Selenate-chloride isotherm 15
Figure 6. Selenate-sulfate isotherm ... .16
Figure 7. Selenite-sulfate isotherm 17
Figure 8. Selenite-nitrate isotherm 18
Figure 9. Graphical determination of selenate breakthrough..... 20
Figure 10. Effect of sulfate on selenate removal 22
Figure 11. Effect of sulfate and nitrate on selenite removal..... 23
Figure 12. Regeneration run effluent concentration history. 25
Figure 13. Removal of selenite by Duolite C-464 in ferric form. 29

Figure A1. Transition types in equilibrium systems 34
Figure A2. Composition-path diagram for a ternary system..... 37
Figure A3. Effect of nitrate on selenite removal. 43
Figure A4. Triangular diagram for the sulfate-nitrate-chloride system 45
Figure A5. Column method for isotherm generation.. 48
Figure A6. Effluent concentration history, Run 2 53
Figure A7. Selenate effluent concentration history, Run 2 54
Figure A8. Effluent concentration history, Run 4 55
Figure A9. Selenate effluent concentration history, Run 4 56
Figure A10. Experimental apparatus. 57

TABLES

Table 1. Chemical data for selenium and sulfur 4
Table 2. Anion retention times on a Dionex Ion Chromatograph 13
Table 3. Summary of separation factors for Dowex 2X8 ... .19
Table 4. Results of column experiments with Dowex 2X8. 24
Table 5. Redox potentials for selenate reduction 27
Table 6. Results of selenate reeduction experiments 27
Table 7. Batch experiments with Duolite C-464 28
Table 8. Representative water composition text example.... 30

Table A1. Selenate-chloride equilibrium data 49
Table A2. Selenate-sulfate equilibrium data 50
Table A3. Selenite-sulfate equilibrium data..... 50
Table A4. Selenite-nitrate equilibrium data 51
Table A5. Chloride-bicarbonate equilibrium data..... 51
Table A6. Column operating data..... 52

ACKNOWLEDGMENTS

We would like to thank the late Professor Theodore Vermeulen for initiating this project with the Environmental Protection Agency and Mr. Richard P. Lauch for his diligence and support throughout. We would also like to thank the staff of the Water Chemical and Thermal Technology Center for their time and efforts and Mr. Raja Tannous and Dr. Richard Fish for the use of the Atomic Absorption Spectrophotometer in the selenium analyses.

List of Symbols

Q Total specific exchanger capacity (meq/g resin)

q_i Concentration of Component i in exchanger (meq/g resin)

y_i Equivalent fraction of Component i in exchanger ($= q_i / Q$)

C_o Total solution concentration (eq/liter solution)

c_i Normality of Component i in solution (eq/l)

x_i Equivalent fraction of Component i in solution ($= c_i / C_o$

α_{ij} Separation factor, defined by Eq. 7

K_{AB} Selectivity coefficient, defined by Eq. 11

ρ_b Bulk density of exchanger (g/ml)

ϵ Void fraction of resin bed (void volume/total bed volume)

v Resin-bed volume (ml)

V Volume of feed solution (ml)

T Throughput parameter, defined by Eq. 13

γ Ratio of equivalent fractions of sulfate and selenate in solution phase ($=x_{SO_4} / x_{SeO_4}$)

m Mass of resin (g)

x_i^o Concentration of Component i feed

SECTION 1

INTRODUCTION

The health effects of selenium are a subject of current medical research. Instances of toxicity as well as nutritional deficiency caused by this element have been reported (1). However, as is the case with many substances required by the body in trace amounts, the level at which selenium becomes toxic has yet to be determined conclusively. Until the role of selenium in human health has been more clearly defined, the Federal Government has, as a precaution, set a maximum contaminent level of 0.01 mg/L selenium on all waters to be used for drinking purposes (2). To comply with this limit, selenium removal is required and suitable methods should be developed to accomodate the wide variation in the chemical form of selenium and in the composition of the waters containing it.

Selenium pollution is not a widespread problem. The relative amount of the element in the crust of the earth is small and deposits rich in selenium are not common. Industrially, selenium is recovered as a by-product of copper refining (3). Nevertheless, in some areas, selenium-rich soils and deposits result in selenium groundwater concentrations several times in excess of the Federal limit. This type of problem was recently observed in a California wildlife refuge (4). Because selenium pollution cases are often local and relatively minor in scale, removal processes should be simple in design and operation as well as reliable, economic and specific.

Past efforts to develop selenium removal-methods have been moderately sucessful. Conventional trace-metal removal methods (such as coagulation and precipitation with lime, alum or iron salts) do not always remove enough selenium to satisfy the Federal maximum concentration limit (5,6). This is due, in part, to the slight solubility of calcium, aluminum, and iron salts of selenite and selenate, the predominant forms of selenium in drinking water. A study by the Environmental Protection Agency in 1980 concluded that activated alumina could remove selenite effectively from drinking water but that selenate removal was limited by the presence of other anions (most notably sulfate) (7). Reverse osmosis was found to be effective but not specific for selenium removal (6,8). Previous studies have shown that ion exchange is a feasible method for selenium removal (5,9,10) but the results are not a sufficient basis for the design of a removal process.

Ion exchange has several features that, in principle, make it suitable for reducing selenium pollution. The removal capacity of an exchanger selective for selenium, in conjunction with low concentrations of selenium in water could be the basis for an effective removal process. The widespread use of domestic water-softening units shows that ion exchange can be used in a wide range of applications. The approach taken in this study was to acquire the critical experimental data from which the merits and limitations of the ion-exchange process could be assessed and to apply the local-equilibrium theory of ion-exchange columns to provide a clear outline of the ion-exchange behavior of selenium.

SECTION 2

CONCLUSIONS AND RECOMMENDATIONS

1) Ion exchange is capable of removing selenium anions (selenate and selenite) from drinking water. The effectiveness of this method depends on the composition of the water. Specifically, for the strong-base resins Dowex 1X8 and 2X8 at representative drinking-water concentrations (around 500 mg/l TDS),

A) Selenate removal is limited only by the presence of sulfate, as the ion exchange behavior of selenate was found to be identical to that of sulfate.

B) Selenite removal is limited by the presence of the sulfate and nitrate anions, which the resins prefer to selenite.

2) Reducing agents suitable for water treatment do not homogeneously reduce selenate to selenite. Under ambient temperature conditions, neither sulfite ion nor zinc metal achieved any reduction of low selenate concentrations. Boiling 4N hydrochloric acid was the only agent examined that accomplished the transformation.

3) Local-equilibrium analysis of fixed-bed ion-exchange columns aided in the interpretation of experimental results and was effective in predicting selenium removal capacities. It provided a theoretical basis on which the relative merits of the ion-exchange process could be evaluated.

4) A weak-acid cation exchanger in the ferric form selecively removed selenate from water that also contained sulfate and chloride. Only preliminary screening experiments were carried out to test this method.

SECTION 3

BACKGROUND INFORMATION

Chemical Aspects

Some background on the relevant chemistry of selenium is helpful for understanding the occurrance of the various forms of selenium in water and how removal processes might effect them. Selenium is a naturally occuring element that can exist in several oxidation states. The two most common forms encountered in drinking waters are the tetravalent selenite ion ($SeO_3^=$) and the hexavalent selenate ion ($SeO_4^=$). Selenium and sulfur belong to the same group in the periodic table and their chemistry, while not identical, is similar. In later sections, this concept will be useful in interpreting experimental results and in applying them to removal-process design. Some chemical data that point to the similarities of these two elements are given in Table 1.

The pK-values shown in the Table have important implications for the ion exchange behavior of the selenium species. In the pH-range normally encountered in drinking waters, selenate as well as sulfate will be in the fully ionized form. On the other hand, the degree of dissociation of selenious acid (between the monovalent biselenite and the divalent selenite forms) in this pH-range is sensitive to pH. The distribution can be estimated from the buffer equation as

$$\log([SeO_3^=] / [HSeO_3^-]) = pH - 7.31 \qquad (1)$$

where [ ] represents the molar concentration of a species. An analogous relation can be found for sulfurous acid by replacing the constant -7.31 by -6.91.

The Table also shows that selenate salts are generally much more soluble than the corresponding selenite salts, an extreme case being the solubility of the ferric salt of each anion. Also, selenite complexes with many common soil components, such as ferric and aluminum sesquioxides (12), and is therefore not easily leached from the soil into groundwater. Selenate, on the other hand, does not form such complexes and thus often represents much of the selenium present in groundwater. These are general conclusions and exceptions can and do occur. A recent review of selenium speciation, distribution and concentration has been given by Robberecht and Van Grieken (13).

TABLE 1. CHEMICAL DATA FOR SELENIUM AND SULFUR

(References 3 and 11)

Dissociation Constants (pK-values) *

Acid	H_2Se	H_2S	H_2SeO_3	H_2SO_3	H_2SeO_4	H_2SO_4
pK_1	3.80	7.04	2.46	1.81	-2.50	-3.00
pK_2	14.0	12.0	7.31	6.91	1.92	1.92

Solubility Products (K_{sp}) **

Cation / Anion	$SeO_3^=$	$SO_3^=$	$SeO_4^=$	$SO_4^=$
Ca^{++}	2.95×10^{-6}	6.8×10^{-8}	9.3×10^{-5}	2.45×10^{-5}
Pb^{++}	3.2×10^{-12}	—	1.6×10^{-7}	1.06×10^{-8}
Ba^{++}	—	—	3.2×10^{-8}	1.00×10^{-10}
Fe^{+++}	2.0×10^{-31}	—	soluble	soluble

*$pK_i = -\log K_i$, where K_i is the ith dissociation constant of the diprotic acid H_2A.

**$K_{sp} = (m)^m(n)^n c_A^m c_B^n$ for the dissociation in water of the slightly soluble salt A_mB_n into ions A^{n+} and B^{m-}.

Basic Concepts For Fixed-Bed Analysis

In this section, concepts useful for the interpretation and prediction of fixed-bed ion-exchange bed behavior are presented. This will serve as a basis for the discussion of experimental results in later sections.

Conventional water treatment by ion exchange consists of the following steps, which, together, constitute the treatment cycle:

Exhaustion: Water, containing impurities to be removed, is passed through the exchanger presaturated (or regenerated) with innocuous, exchangeable counterions (which, in the present case, would probably be the chloride ion). These ions are exchanged for those in the feed so that the undesired anionic species are removed. The process is continued until the capacity of the bed is reached, such as when an undesireable species in the feed reaches the maximum acceptable level in the column effluent. At this point, the bed is considered to be exhausted.

Regeneration: The exhausted bed is restored to its original form by regenerating it with a solution containing only the presaturating ion. The impurities displaced from the bed are disposed of and the cycle is begun again.

Minor additional steps in a cycle, such as rinsing and backwashing, are not included in a preliminary process design and are not considered here.

As an example, consider the treatment of a feed water containing sulfate, nitrate and chloride by a strong base anion exchanger in the chloride form. As the steps shown above proceed, the composition of the column effluent varies as shown in the effluent concentration history of Figure 1. Practical design of an ion-exchange treatment system requires realistic prediction of such a history.

Equilibrium Behavior And Models

Ion exchange, as considered here, conserves the total solution normality (C_o). Expressing concentrations in the fluid-phase (c_i) in normalities and the concentrations in the resin-phase (q_i) in ion-equivalents per kilogram of resin, this conservation statement may be expressed as,

$$\sum_{i=1}^{n} c_i = C_o \tag{2}$$

$$\sum_{i=1}^{n} q_i = Q \tag{3}$$

where Q is the total resin capacity and n the total number of exchangeable species in the mixture. Division of Eq. (2) by C_o and of Eq. (3) by Q gives the equivalent statements.

$$\sum_{i=1}^{n} x_i = 1 \tag{4}$$

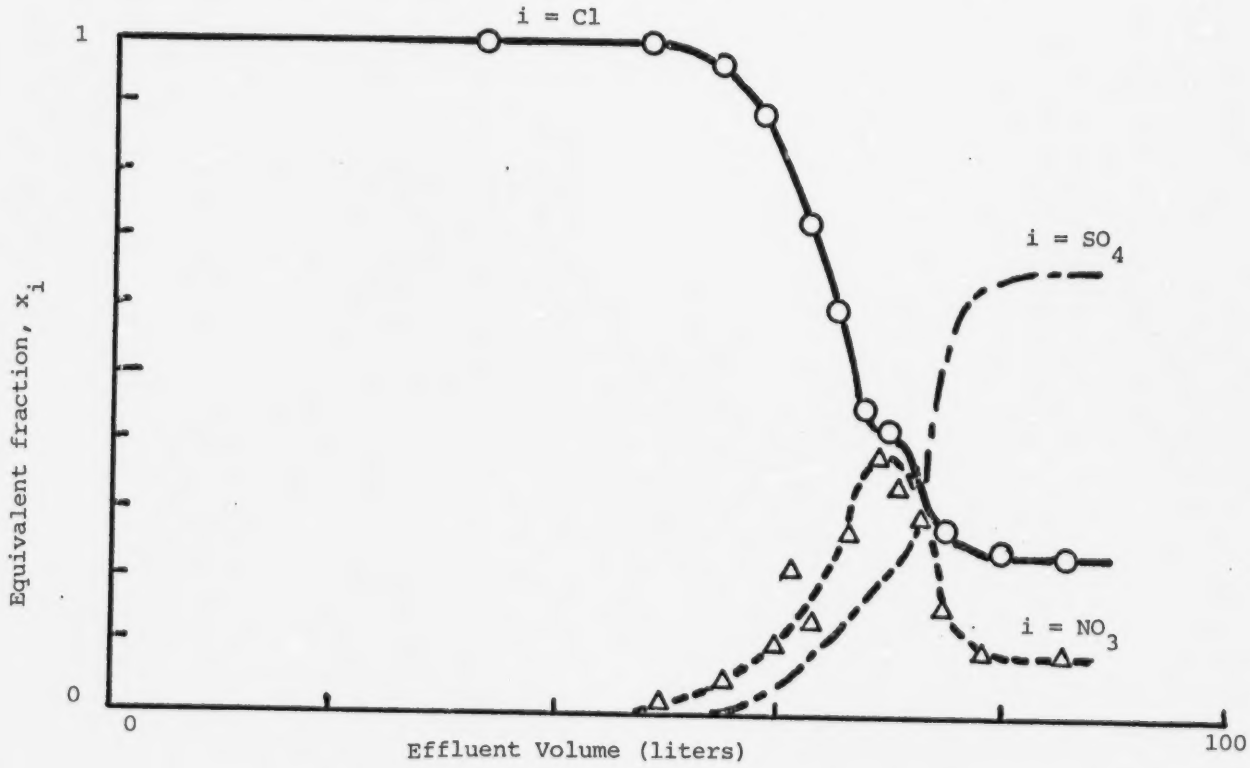

Figure 1. Effluent-concentration history for feed composition $x_{SO_4} = 0.7$, $x_{Cl} = 0.2$, and $x_{NO_3} = 0.1$ at $C_o = 0.0033$ N. Bed of 150 ml Duolite A101D initially presaturated with chloride. Flowrate; 150 ml/min. Sulfate curve by difference. (Reference 14)

$$\sum_{i=1}^{n} y_i = 1 \tag{5}$$

where $x_i = c_i / C_o$ and $y_i = q_i / Q$ are the respective fluid- and resin-phase equivalent fractions of exchangeable species i.

The resin-phase fractions are related to the fluid-phase fractions by an equilibrium isotherm. In general, the isotherm for an n-component mixture can be represented by a set of n-1 independent equations

$$y_i = F_i(x_1, x_2, \ldots, x_n) \tag{6}$$

A binary isotherm is considered favorable for uptake of a particular component if the ratio of its resin phase to its fluid phase fractions (y_i / x_i) is greater than unity for all values of x_i. Unfavorability implies that this ratio is less than unity and for a linear isotherm, it is unity. Examples of these types of isotherms are shown in Figure 2.

The functions of Eqs. 6 are usually represented by simple yet sufficiently realistic mathematical models, such as the constant-separation-factor model. This model has been extensively used in this study for correlation of data and prediction of behavior. It can be shown that this model describes a hyperbolic isotherm and is equivalent to the Langmuir adsorption isotherm (15). For a mixture of two components, i and j, the separation factor, α_{ij}, is defined as,

$$\alpha_{ij} = (y_i / x_i)(x_j / y_j) = 1 / \alpha_{ji} \tag{7}$$

A value of α_{ij} greater than unity indicates preference by the resin (favorability of uptake) for species i over species j. Also, in a mixture of any number of components, the following relation holds for any three species i, j and k;

$$\alpha_{ij} = \alpha_{ik} \alpha_{kj} \tag{8}$$

Because the constant separation factor model represents the equilibrium properties of an n-component system through a set of n-1 binary parameters (α_{ij}), it affords considerable reduction in the theoretical and experimental work required to use the model. A plot of the isotherm represented by this model for a binary system is shown in Figure 2. Additional relations for this model may be found in Appendix A1.

By referencing all the α_{ij} -values for an n-component mixture to the most strongly held component of that mixture (taken to be Component 1), the separation factors can be arranged in the sequence,

$$1 = \alpha_{11} < \alpha_{12} < \alpha_{13} < \cdots < \alpha_{1n} \tag{9}$$

This is termed the selectivity sequence for a mixture and is useful for predicting general features of the ion-exchange process (see Appendix A1).

As noted above, the constant-separation-factor model provides a simple means of representing the equilibrium properties of a mixture. However, this model is not without limitations. Changes in total solution normality can alter the selectivity sequence, particularly in the case of heterovalent exchange (exchange of ions of unlike charge). A model which does predict this variation is the so-called mass-action model. It is developed by postulating the exchange between ions A and B;

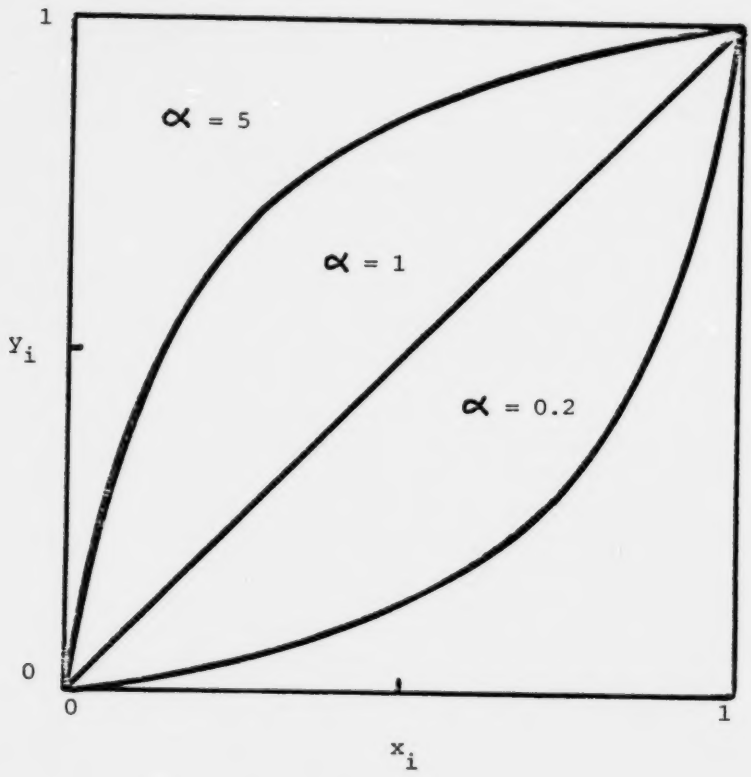

Figure 2. Constant-separation-factor isotherms for binary system (See Eq. 7). $\alpha > 1, < 1$ or = 1 corresponds to favorable, unfavorable and linear isotherms.

$$bA^{a} + aR_{b}\,B \qquad aB^{b} + bR_{a}\,A \tag{10}$$

where a and b are the respective valences for species A and B, and R stands for a resin site. Assuming that the activity coefficients are unity, an equilibrium constant for this reaction can be written as,

$$K_{AB} = (y_A / x_A)^{b}\ (x_B / y_B)^{a}\ (Q / C_o)^{b-a} \tag{11}$$

K_{AB} is termed the selectivity coefficient for the exchange. For homovalent exchange (a = b), this model reduces to the constant separation factor model. For heterovalent exchange, a≠ b, so that Eq. 11 shows that the total solution concentration, C_o , becomes a factor in determining the selectivity. For example, in the sulfate-chloride exchange, a = 2 and b = 1 so that Eq. 11 becomes

$$K_{SO_4,Cl} = (y_{SO_4} / x_{SO_4})\,(x_{Cl} / y_{Cl})^{2}\,(C_o / Q) \tag{12}$$

Equation 12 predicts, for a given fluid phase composition (x_{SO_4} and x_{Cl}), that as the total solution concentration (C_o) is increased, y_{SO_4} / y_{Cl} must decrease in order to keep $K_{SO_4,Cl}$ constant. Thus, the resin increases its preference for chloride in more concentrated solutions, a circumstance that is used to increase the utilization of monovalent regenerant ions. This effect of the total concentration on the isotherm is termed the "electroselectivity" effect (16) and is illustrated in Figure 3.

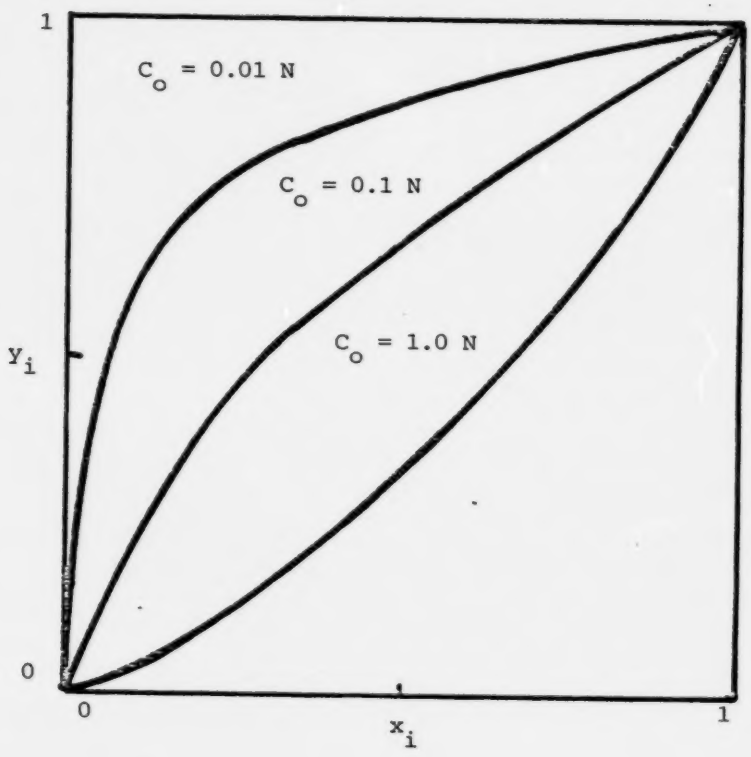

Figure 3. Effect of total solution concentration on a divalent-monovalent isotherm (cf. Eq. 10) with $K_{AB}Q$ = 0.33 N. Increase in C_o decreases the selectivity for the divalent ion (A).

Column Behavior

One of the simplest theories linking the equilibrium isotherm to prediction of fixed-bed performance is the so-called local-equilibrium theory. This theory was stated comprehensively for two-component systems by DeVault (17) and later developed for to multicomponent systems by Klein, et.al (18), Tondeur (19), Helfferich and Klein (15), and Rhee, et.al. (20).

The local-equilibrium theory assumes the absence of mass-transfer inefficiencies and bases its predictions of axial concentration profiles and effluent concentration histories solely on the equilibrium properties of the system. More elaborate treatments can account for the rate effects in real systems but they incur a considerable increase in calculational complexity and require numerous additional parameters. The local-equilibrium theory, on the other hand, predicts the behavior of a real system only qualitatively but in a simple and clear manner. This advantage is particularly valuable for multicomponent systems.

Prediction of an effluent-concentration history for an n-component system is not readily possible for a system as represented by the arbitrary isotherm functions of Eqs. 6. However, as is shown in References 15 and 18 through 20, the constant-separation-factor model provides a solution that can be quite general in its interpretation and application. This model was used here in conjunction with the local-equilibrium theory to guide planning of experiments and to interpret their results.

The effluent-concentration history shown in Figure 1 is that of a real system and therefore reflects the effect of mass-transfer inefficiencies. The effluent concentration history predicted by the local-equilibrium theory for the same system is shown in Figure 4. Because of the simplifying premises adopted by the theory, the predicted effluent concentration history exhibits sharp steps rather than the gradual curves seen in Figure 1. Though the theory does not reflect the detailed behavior of the real system, it does qualitatively predict the overall sequence of changes in the column effluent composition with effluent volume.

The mathematical treatment of fixed-bed behavior is greatly simplified by introducing the throughput parameter, T, defined as,

$$T = \frac{C_o\ (V\ -\epsilon v)}{\rho_b Q\ v} \tag{13}$$

where V is the volume of effluent passed through the bed, v the bed volume, ϵ the void fraction of the bed, and ρ_b the bulk density of the resin. Since, at a constant flow rate, V is proportional to time, Eq. 13 transforms time into a dimensionless time variable, T (for a given bed volume). The throughput parameter corresponds to the ratio of the equivalents of solution leaving a column, $C_o\ (V\ -\epsilon v)$, to the number of equivalents held by the bed, $\rho_b Q\ v$, and is thus a measure of capacity as can be seen from the relation,

$$\frac{V}{v} = \frac{\rho_b Q}{C_o} T + \epsilon \tag{14}$$

where $V\ /\ v$ is the number of bed volumes of feed. Under normal circumstances, the ϵ term can be neglected.

Further details on ion-exchange column behavior under the premises of the local-equilibrium theory are given in Appendix A1.

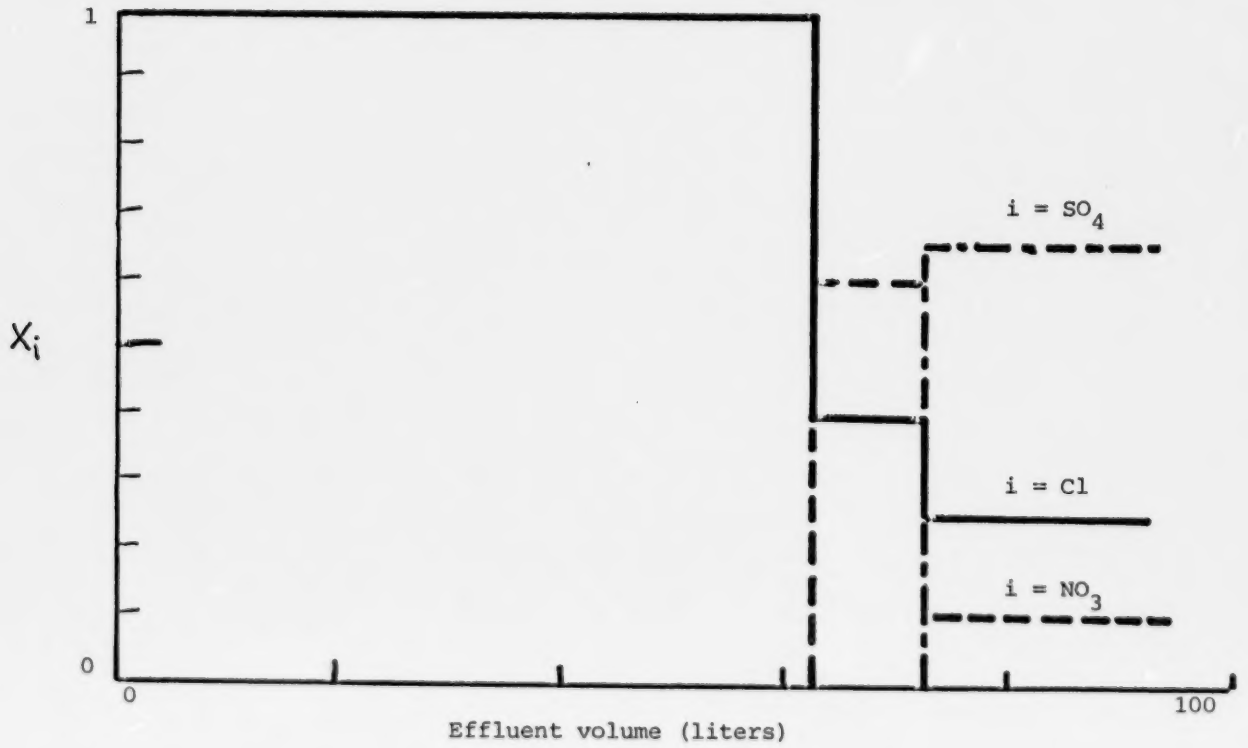

Figure 4. Effluent-concentration history for system of Fig. 1, as predicted by local-equilibrium theory with constant separation factors $\alpha_{SO_4,NO_3} = 9$, $\alpha_{SO_4,NO_3} = 3$.

SECTION 4

SELENIUM REMOVAL STUDY

The following sections review and discuss the results of the present study. An effort was made to show the behavior of selenium anions relative to the anions commonly present in water (sulfate, chloride, and bicarbonate).

Ion Exchange Equilibria Involving Selenium

Equilibrium data on the exchange of selenium ions (e.g., separation constants) in the presence of common drinking-water anions (such as sulfate, chloride, bicarbonate or nitrate) are sparse in the published literature. No studies have been found that provide data useful for the design and evaluation of ion exchange methods for selenium removal.

Some data from a recent ion-chromatographic study by Williams (21) do offer some insight into the exchange behavior of selenium relative to other inorganic ions. Twenty-seven anions were analyzed with an ion chromatograph, using a carbonate-bicarbonate mixture as eluent and presaturant. The data of greatest interest are summarized in Table 2.

TABLE 2. ANION RETENTION TIMES ON A DIONEX ION CHROMATOGRAPH (21) *

Eluent - 0.003 M $NaHCO_3$ and 0.0024 M Na_2CO_3

Anion	Cl^-	$SeO_3^=$	NO_3^-	$SO_4^=$	$SeO_4^=$
Retention Time (min)	4.6	6.9	15.2	22.8	27.2

* Dionex is a registered trademark of the Dionex Corporation.

From the trace principle (see Appendix A1), it can be shown that the velocity at which a trace concentration of an ion moves through a bed of ion-exchange resin is inversely proportional to the selectivity of the exchanger for that ion. In ion chromatography, this translates to higher retention times for species with higher separation factors relative to the eluting medium. With this in mind, the properties of the constant-separation-factor model (Eqs. 7 and 8) can be used to create the following order of separation factors from the data of Table 2:

$$\alpha_{SeO_4,SO_4} < 1 = \alpha_{SO_4,SO_4} < \alpha_{SO_4,NO_3} < \alpha_{SO_4,SeO_3} < \alpha_{SO_4,Cl} \qquad (15)$$

Similar results have been reported by Hoover and Yager (22).

As the total solution concentration (0.008 N) used in Williams' study is in the range of normal drinking waters, these retention time data allow a preliminary assessment of the ion-exchange behavior of selenium and the consequences of this behavior for selenium removal from drinking waters. Of the anions involved in this study, selenate and sulfate were the most strongly preferred by the resin used. This indicates that ion exchange could have a high capacity for selenate removal since the resin has such a high preference for the ion over all the others. However, the resin is not as selective for selenite as both sulfate and nitrate are held more tightly. Thus, selenite will suffer more interference in its removal by ion exchange. These points will be elaborated upon below.

For the present study, the separation factors needed to describe the six-component system comprising sulfate, nitrate, chloride, bicarbonate, selenite and selenate were determined experimentally or were taken from literature data. All recorded data and descriptions of experimental methods are presented in Appendix A4. Figs. 5 through 8 summarize the experimental results.

Figure 5: Selenate-chloride exchange - Curves 2 and 3 on this Figure shows that at the low total concentrations of interest, drinking water concentrations below 0.01 N, the selectivity for selenate over chloride is very high ($\alpha_{SeO_4,Cl} \approx$ 10 to 20). This is a heterovalent exchange and, as expected, the total solution concentration plays an important role in determining the degree of resin selectivity.

Figure 6: Selenate-sulfate isotherm - This Figure shows that for this system, the isotherm is linear so that $\alpha_{SeO_4,SO_4} = 1.0$. Neither ion is preferred by the exchanger over the other and the two species can be combined and treated effectively as one.

Figure 7: Selenite-sulfate exchange- Both Dowex 1 and Dowex 2 significantly prefer sulfate to selenite since $\alpha_{SeO_3,SO_4} = 0.2$ (or $\alpha_{SO_4,SeO_3} = 1 / \alpha_{SeO_3,SO_4} = 5.0$).

Figure 8: Selenite-nitrate exchange- This isotherm shows a slight preference towards nitrate with $\alpha_{SeO_3,NO_3} = 0.8$. Since this is a heterovalent exchange, the total solution concentration may again be expected to be a determining factor in the selectivity of the resin with the selectivity for nitrate increasing with concentration.

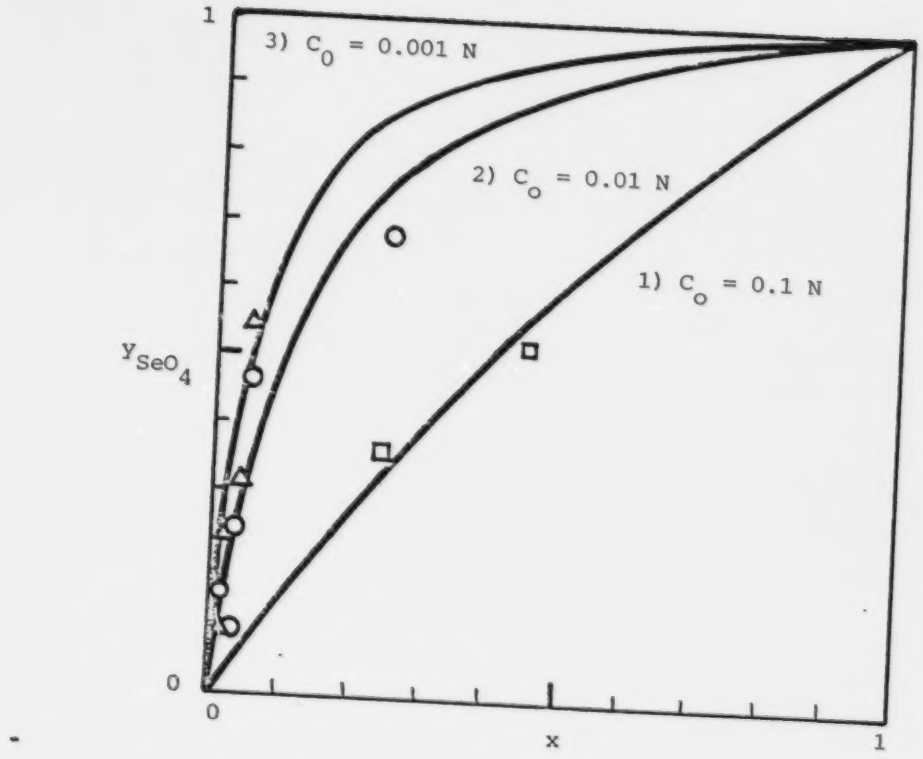

Figure 5. Effect of total solution concentration on selenate-chloride isotherm for Dowex 2X8. For C_o = 0.001, 0.01 and 0.1, $\alpha_{SeO_4,Cl}$ = 18.7, 9.6 and 1.5, respectively.

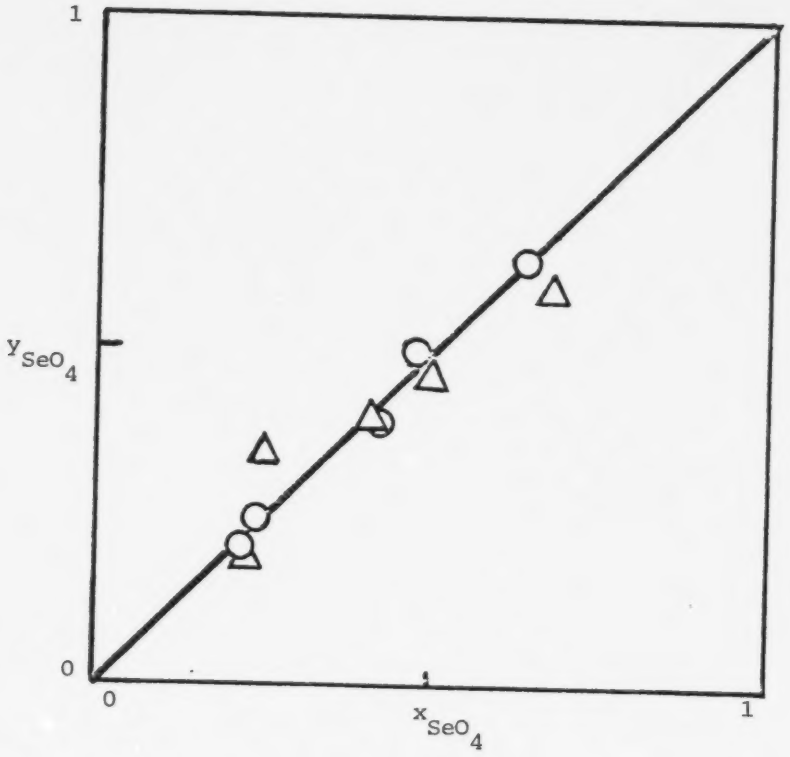

Figure 6. Selenate-sulfate isotherm for Dowex 1X8 (Δ) and Dowex 2X8 (o). C_o = 0.01 N, pH = 7.

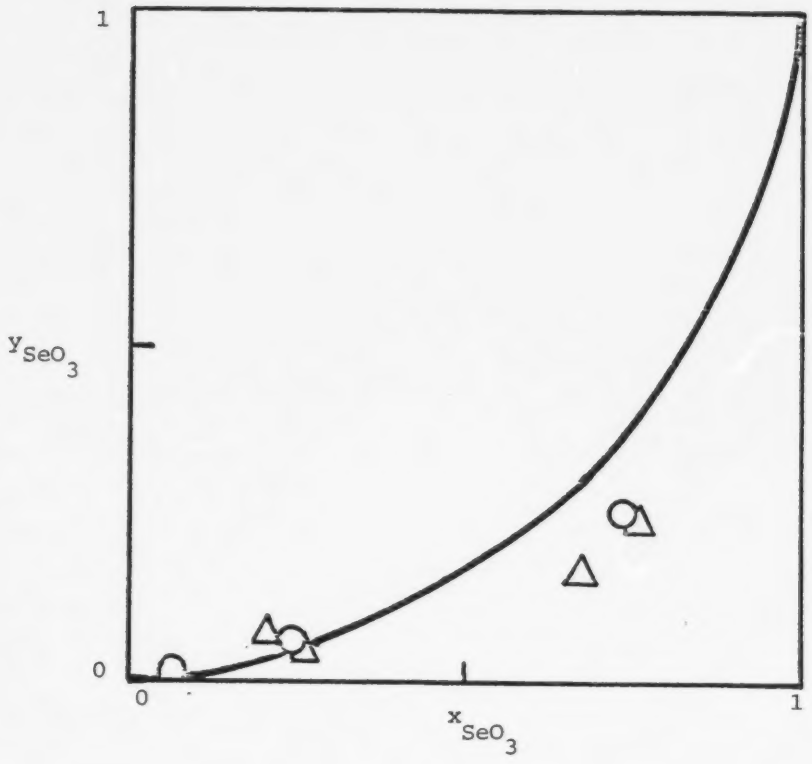

Figure 7. Selenite-sulfate isotherm for Dowex 1X8 (Δ) and Dowex 2X8 (o). C_o = 0.05 to 0.1 N, pH = 9.

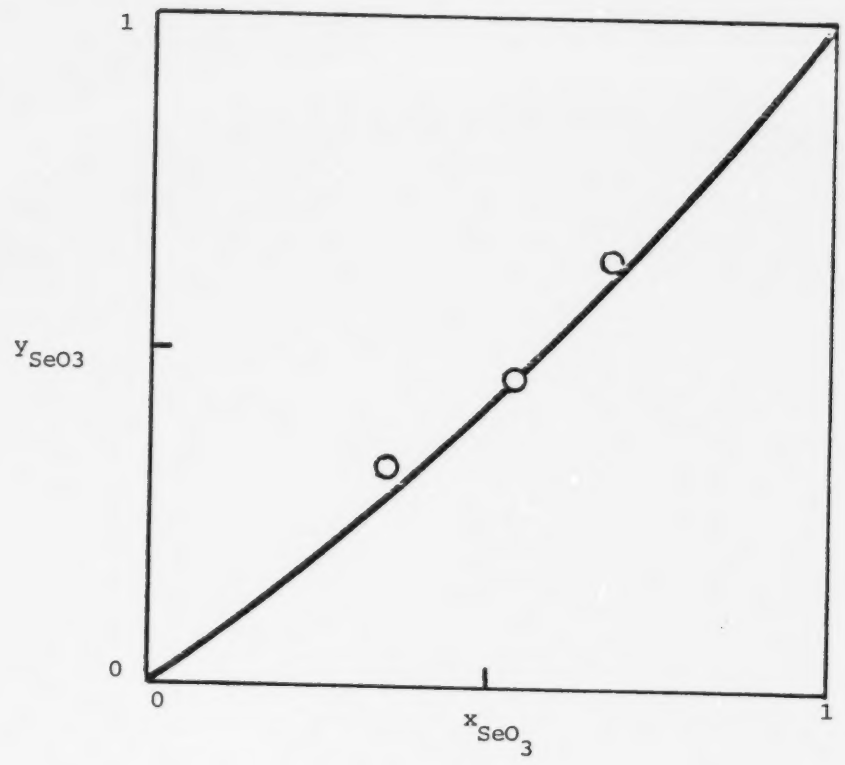

Figure 8. Selenite-nitrate isotherm for Dowex 2X8. C_o = 0.005 N, pH = 8.

Utilization of Equilibrium Data for Performance Prediction

These experimental results, along with supplemental data from the literature, can be used to quantify the selectivity sequence of Eq. 15. The result is presented in Table 3.

TABLE 3. SUMMARY OF RELEVANT SEPARATION FACTORS FOR DOWEX 2X8 AT C_o = 0.005 N

Anion, X	$SeO_4^=$	NO_3^-	$SeO_3^=$	Cl^-	HCO_3^-
$\alpha_{SO_4,X}$	1.0	3.0	5.0	20.0	75.0

The entries in the Table can be used in conjunction with Eq. 8 and the local-equilibrium theory to establish the utility of ion exchange for selenium removal. As Table 3 shows, selenium species are not preferred by typical strong base resins over all the common anions in water. The presence of these anions will limit selenium removal. However, this limitation will not be the same for selenate as for selenite.

At drinking-water concentrations, selenate is preferred by the resin to all other common anions except sulfate. Hence, in the absence of sulfate, ion exchange provides a highly effective means of selenate removal (in terms of bed volumes that can be treated per cycle and in terms of ion-exchange resin used per unit amount of selenate removed).

However, the linearity of the selenate-sulfate isotherm (Fig. 6) means that the resin will not be able to achieve any separation of a mixture of these anions. The ratio of their resin-phase fractions will always be equal to that of their fluid-phase fractions, regardless of the solution composition (see Eq. 7). Since this is a homovalent exchange, solution concentration will not have a large effect on the selectivity. Throughout the ion-exchange process, selenate and sulfate will remain together with equal fractions of each ion being removed at the same time. For example, removing 90 percent of the selenate in a water requires simultaneous removal of 90 percent of the sulfate in that water. But because sulfate concentrations in drinking water are normally so much higher than those of selenate, a bed of resin will have most of its (fixed) capacity taken up by sulfate at the time that the combined selenate-sulfate fraction saturates the bed. Though this affords simplifications for process design in that the capacity for selenium removal can be determined from the capacity for sulfate removal, it indicates that ion exchange will not be as efficient in removing selenate from high-sulfate concentration waters.

Figures 9 and 10 illustrate the effect of sulfate on selenate removal. The details behind these Figures are discussed in Appendices A2 and A3. Figure 9 is a nomograph for determining the T-value (and hence the capacity - see Eq. 14) at which selenate breaks through directly from the selenate-chloride isotherm. The prediction is based on the local equilibrium theory and applies to beds presaturated with chloride and recieving a mixture of selenate and chloride. Normally, selenate concentrations in drinking waters are quite low (100 ppb Se as $SeO_4^=$ translates to a selenate feed fraction, $x^o_{SeO_4}$, of 0.0005 at a total concentration of 0.005 N) and, in the absence of sulfate, the trace principle (see Appendix A1), predicts that the value of T at which selenate emerges from the bed will be large, approaching the value of $\alpha_{SeO_4,Cl}$.

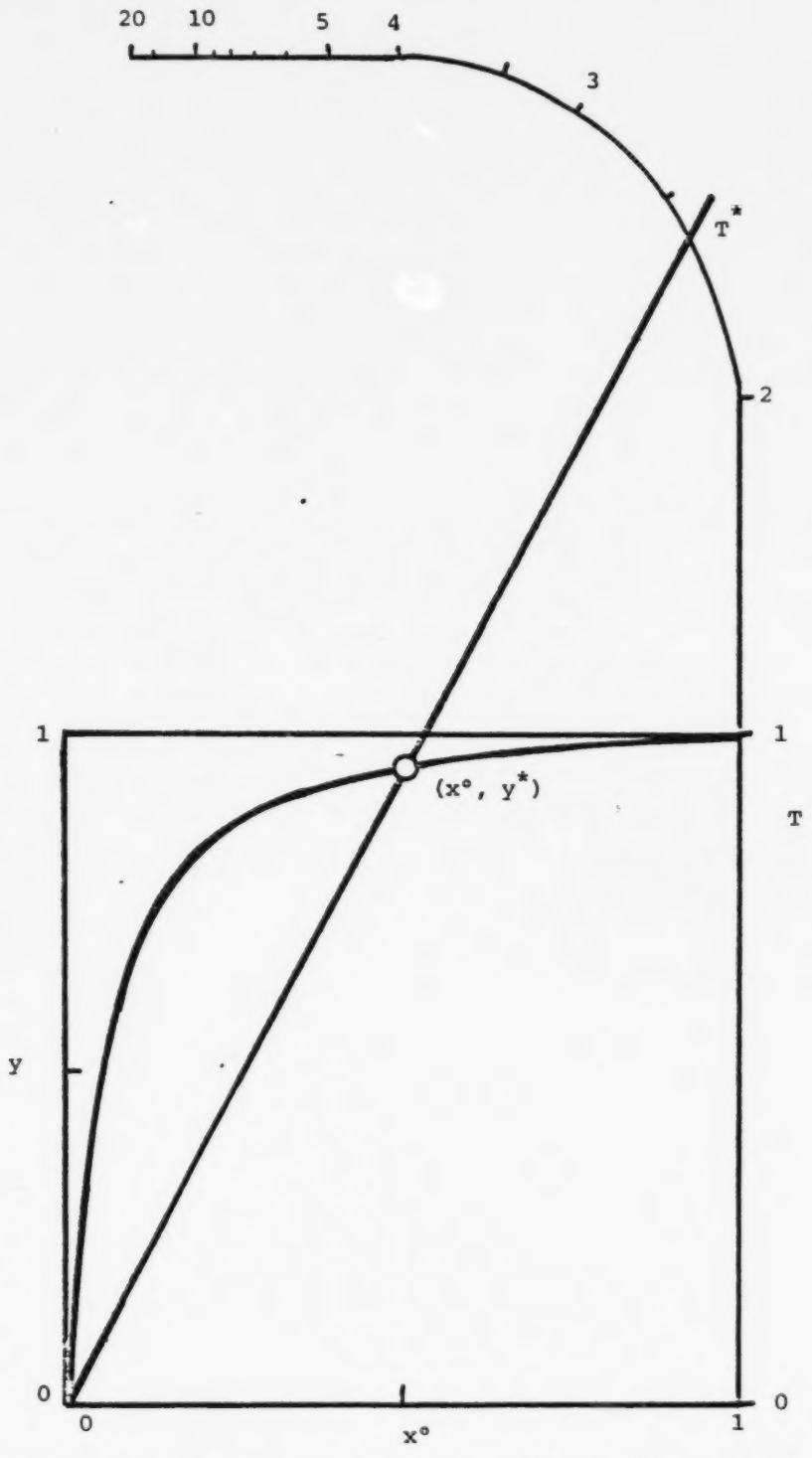

Figure 9. Selenate breakthrough for selenate-sulfate-chloride feed and bed initially in chloride form. Line through (x°,y*) and origin intersects T-curve at breakthrough value (T*). x° and y are combined selenate-sulfate equivalent fractions (e.g., $x^\circ = x^\circ_{SeO_4} + x^\circ_{SO_4}$).

Addition of sulfate increases the number of components to three but since $\alpha_{SeO_4 SO_4} = 1.0$, the mixture can still be treated as a two component system (chloride and the combined selenate-sulfate fraction). As more sulfate is added relative to selenate (keeping the total concentration constant), the effective fraction of selenate in the feed ($x^\circ = x^\circ_{SeO_4} + x^\circ_{SO_4}$) increases and from Figure 9, the T-value at breakthrough approaches unity. The capacity of a bed for removal of selenate is thus controlled by changes in sulfate concentration since low selenate concentrations do little to change the combined selenate-sulfate fraction in most drinking waters. The effect of sulfate and total solution normality on selenate removal (as predicted from equilibrium theory) from selenate-sulfate-chloride mixtures by Dowex 2X8 in the chloride form, is shown in Figure 10.

As a consequence of its position in the selectivity sequence outlined in Table 3, selenite removal by ion exchange will be limited by sulfate and nitrate. Since both of these anions are preferred to selenite, a bed of resin will still hold these species when selenite breaks through the column and thereby reduce a bed's capacity to remove selenite. Figure 11 presents a summary of these effects as predicted by the local-equilibrium theory. Background for this Figure is presented in Appendix A3. Comparison of Figures 10 and 11 shows that selenite removal is more limited by the presence of other anions than selenate is.

Another factor in the ion-exchange removal of selenite is the pH of the water to be treated. At neutral pH, tetravalent selenium is half in the monovalent biselenite form and half in the divalent selenite form (see Eq. 1). Hence, the ion-exchange behavior of both these species should be considered. However, the monovalent biselenite should be less preferred than the divalent selenite (see Basic Concepts for Fixed-Bed Analysis in Section 3) and so this study ignored the presence of biselenite.

The results shown in Figures 10 and 11 are of prime importance when considering ion exchange for selenium removal. Though both species of selenium can be removed by ion-exchange resins, removal efficiency of selenate is potentially higher than that for selenite. Additionally, the removal of both species is determined more by the gross composition of water (specifically, the nitrate and sulfate levels) than by the absolute concentrations of the selenium species themselves.

The efforts of this study have focussed on the use of strong-base resins. Weak-base resins were not examined due to time constraints. Also, because weak-base resins require alkali for regeneration, they were not considered practical for small-scale applications.

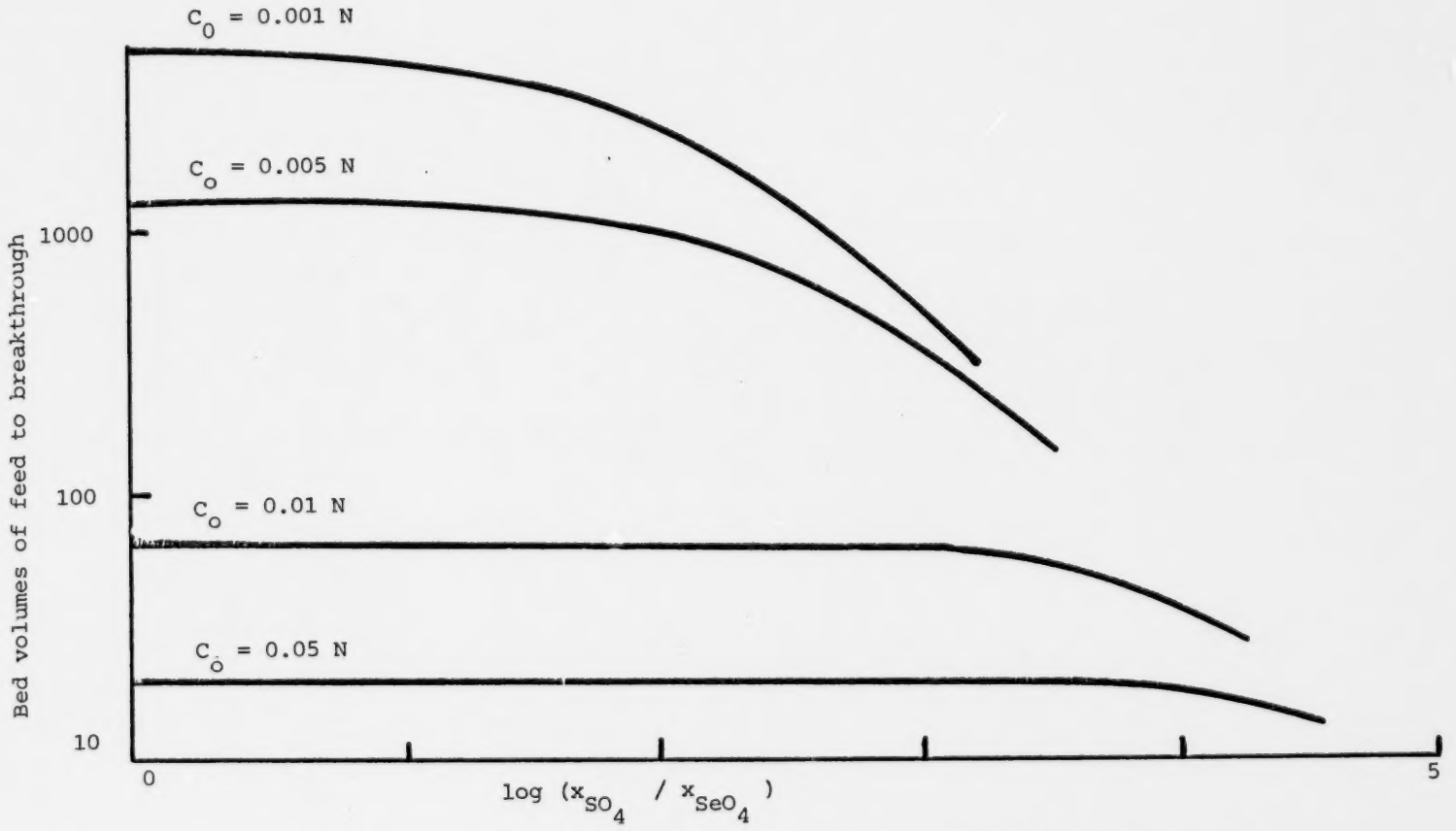

Figure 10. Effect of sulfate-selenate ratio on selenate removal for feeds containing 50 ppb selenium and bed initially in chloride form. Prediction from local-equilibrium theory. Resin: Dowex 2X8 ($_bQ$ = 1.3 meq/ml).

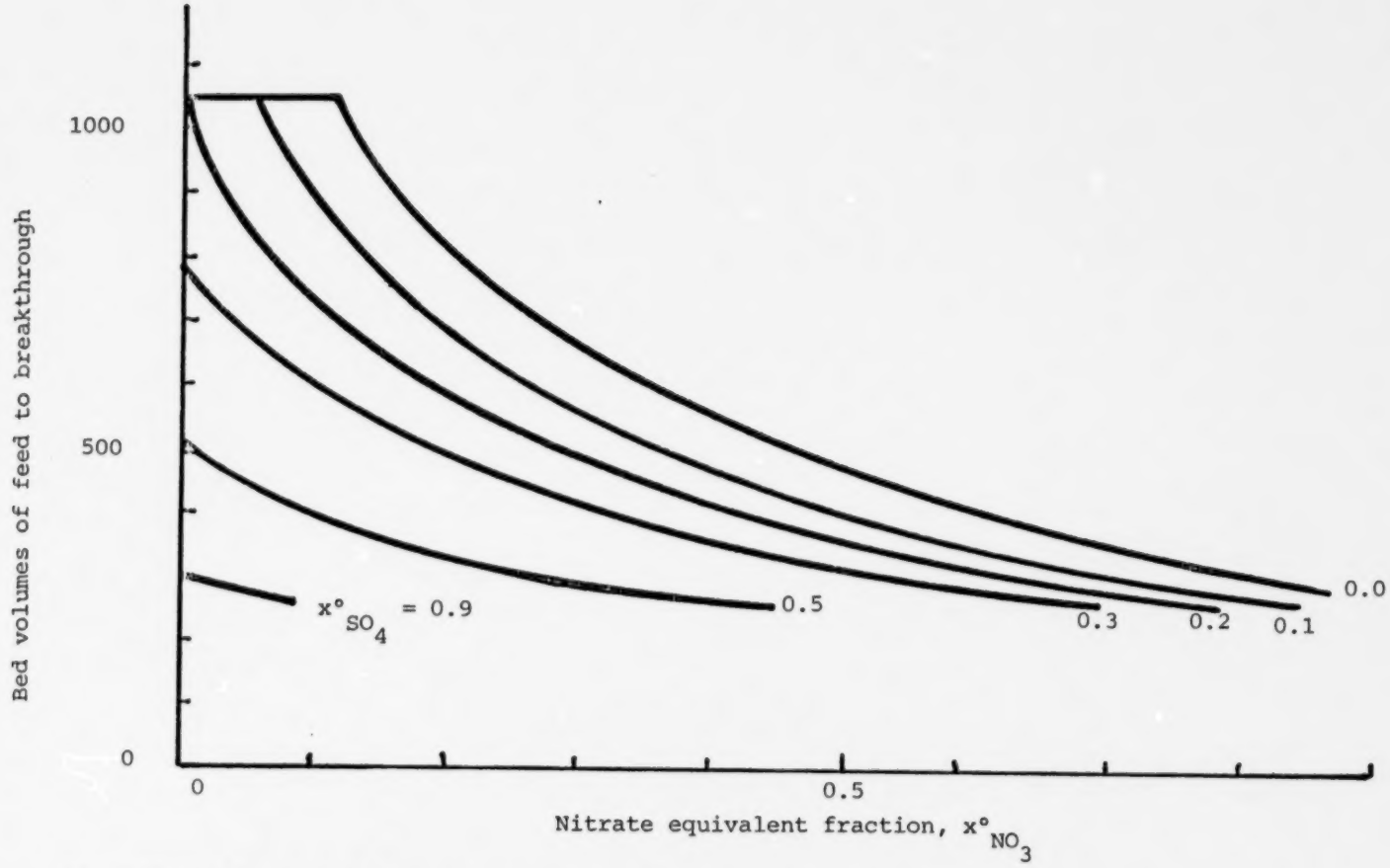

Figure 11. Effect of composition on breakthrough capacity for removal of selenite by Dowex 2X8 in the chloride form. Feeds contain sulfate, nitrate and chloride at C_o = 0.005 N.

Column Studies

Column runs were conducted to verify some of the predictions made in the previous Section on Utilization of Equilibrium Data for Performance Prediction. Table 4 summarizes the results of this portion of the study and compares theory and experiment. A full record of the experimental apparatus, procedures and conditions is provided in Appendix A5. Equations used for prediction and an example of a predicted capacity are given in Appendix A2.

TABLE 4. RESULTS OF COLUMN EXPERIMENTS WITH DOWEX 2X8

Run*	Feed Composition				Capacity for Se(VI) in Bed Volumes of Feed	
	C_{SO_4} (ppm)	C_{Cl} (ppm)	C_{HCO_3} (ppm)	C_{SeO_4} (ppb Se)	Predicted	Actual
1	192	34	26	50	320	345
2	110	31	140	40	570	614
3	250	0	0	80	300	278
4	120	89	0	90	690	665
5	25	160	0	100	1864	1817

* Runs 1 and 2: resin in bicarbonate form, Runs 3 through 5: resin in chloride form.

Exhaustion Runs

For these runs, feeds containing selenate and several other common anions were passed through beds that were either in the chloride or bicarbonate form. As shown in Table 4, experimental results were in good agreement with theoretical predictions, especially for the chloride-presaturant runs. Comments on experimental difficulties may be found in Appendix A5.

These runs reinforce the equilibrium result that selenate follows sulfate through the removal process. Quantitative study of kinetic effects in the removal of selenate was not undertaken in this study. Due to the unfavorable equilibria for selenite removal, no column runs were conducted that involved this species.

Regeneration Runs

To follow the fate of selenate and sulfate through the regeneration process, a regeneration run was undertaken. A single run was considered sufficient since it confirmed the inability of Dowex 2X8 to discriminate between selenate and sulfate. The bed was uniformly presaturated with a selenate-sulfate mixture and regeneration effected with a 0.1 N solution of sodium chloride. Figure 12 shows the results and confirms the similarity of sulfate and selenate as well as the utility of the local-equilibrium theory in predicting fixed-bed performance.

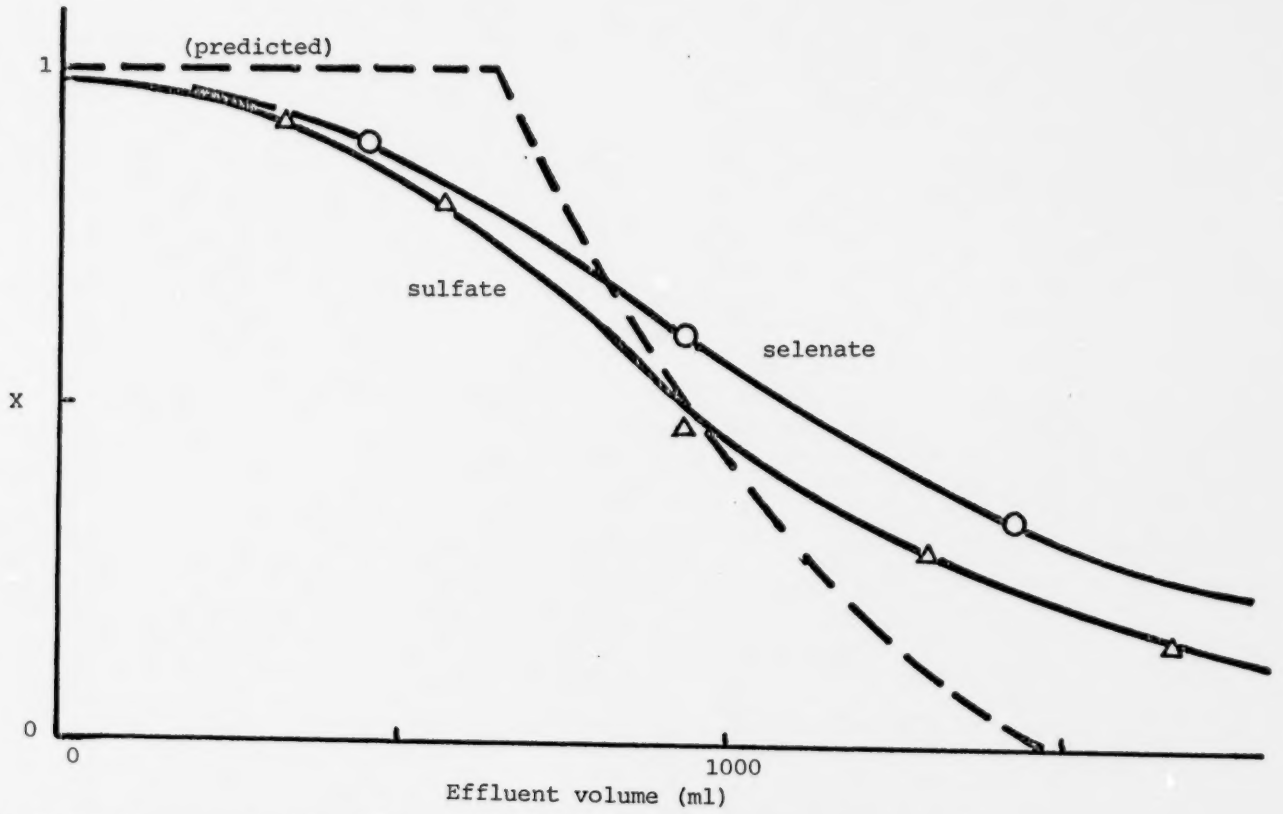

Figure 12. Effluent-concentration history for selenate and sulfate regeneration with 0.1 N NaCl. X is the fractional change in sulfate or sulfate normality during course of experiment. For experimental conditions, cf. Appendix A5. History predicted by equilibrium theory shown for comparison.

Novel Removal Techniques

As an alternative to selenium removal by ion exchange, one may consider the chemical reduction of selenate to selenite. If the reduction could be achieved, the selective removal properties of alumina (7) could be employed to remove all selenium as selenite.

Agents capable of reducing selenate on the scale required for water treatment should have the following properties:

1) Their use should not create more problems than they solve. Their oxidized states should either be acceptable in drinking water or be easily removed from it.
2) They should be chemically very active because selenium is normally present in minute concentrations in water.
3) They should be selective in achieving reduction. They should neither reduce the selenate all the way to the highly toxic selenide form ($Se^{=}$) nor waste reducing power by reducing other materials in water (e.g., organics, other metals).

A summary of information on the electrochemical behavior of selenium and some other common reducing agents is presented in Table 5. The redox couples shown there were chosen both because their oxidation potentials were sufficiently large to achieve the reduction of selenate and because, at moderate levels, their oxidation products can be considered innocuous in drinking water.

Literature data on the interconversion of the various selenium oxidation states (selenide through selenate) suggest the following observations:

1) Selenite can be reduced to elemental selenium or selenide by a number of reducing agents, such as ascorbic acid (23), sodium borohydride (24), hydrazine (25) and sulfur dioxide gas (26).
2) Oxidation of selenite to selenate is somewhat slow and often requires elevated temperatures and high concentration of reagents such as hydrogen peroxide (27), cerium(IV) (28) and chlorine gas (29).
3) Reduction of selenate to selenite takes place at high temperature and reagent concentration (30).

The data suggest that the conversion of selenate to selenite might be quite difficult under mild conditions. Experiments performed in this study have borne out this conclusion. The results are summarized in Table 6. Of the three reagents used, only the most severe (and also the least applicable to large-scale water treatment) proved effective. Though the present study is not exhaustive, it does indicate that homogeneous selenate-reduction methods are likely to be inapplicable to water treatment.

TABLE 5. SELECTED STANDARD REDOX POTENTIALS PERTINENT TO SELENATE REDUCTION (3)

Half Cell	V° (volts)
1) $SeO_4^{=} + H_2O + 2e^- \quad SeO_3^{=} + 2OH^-$	0.03
2) $SO_4^{=} + H_2O + 2e^- \quad SO_3^{=} + 2OH^-$	-0.93
3) $Mg^{++} + 2e^- \quad Mg$	-2.375
4) $Zn^{++} + 2e^- \quad Zn$	-0.7628
5) $Fe^{++} + 2e^- \quad Fe$	-0.440

Note: $\Delta G^\circ = nFV^\circ$ where n is the number of electrons transferred in the reaction, F is Faraday's constant and ΔG° is the standard Gibbs free energy change.

TABLE 6. RESULTS OF SELENATE REDUCTION EXPERIMENTS

Reducing Agent or Couple	Conditions	Results
$Zn - Zn^{++}$	98 μg Se (as $SeO_4^{=}$) and 112 mg Zn metal dust in 200 ml water at 20 °C.	No reduction after twenty-four hours
$SO_3^{=} - SO_4^{=}$	74 μg Se (as $SeO_4^{=}$) and 0.26 g $NaHSO_3$ in 200 ml water at 22 °C, pH 2.5.	No reduction after seventy-two hours.
	134 μg Se (as $SeO_4^{=}$) and 0.26 g $NaHSO_3$ in 200 ml water at 73 °C, pH 2.7.	No reduction after twenty-four hours.
4N HCl	35 μg Se (as $SeO_4^{=}$) boiled at 100 °C in 4N HCl.	Complete reduction after 30 minutes.

Additionally, exploratory experiments were conducted to test the technical feasibility of a novel method for selenite removal. This method took advantage of the insolubility of ferric selenite (see Table 1). A weak-acid cation exchanger in the ferric form was used as material selective for selenite over sulfate, chloride and other common anions.

In neutral to alkaline solutions of low total concentrations, weak-acid cation exchangers hold multi-valent ions strongly in preference to the monovalent sodium ion. Hence, passing a solution of, say, sodium chloride through a bed of this exchanger in the ferric form would only slowly displace the iron from the resin. If selenite ions were present in the solution, the iron liberated by exchange with sodium could precipitate with the selenite. Thus, the resin would act as a continuous dosing agent. Similar investigations in the past dealing with this idea have been applied to sea-water desalination (31,32) but not to selenium removal. No attempt was made here to produce a full analysis of the process. Only exploratory experiments were conducted to test the technical feasibility of the idea.

Batch equilibrium experiments were conducted with a weak-acid exchanger (Duolite C-464) in the ferric form (for selenite removal) and barium ions (for selenate removal). The results of these experiments, summarized in Table 7, show that the iron-selenite system holds the greatest promise.

TABLE 7. BATCH EQUILIBRIUM EXPERIMENTS WITH DUOLITE C-464 WEAK-ACID RESIN IN BARIUM AND FERRIC FORMS.

Initial Selenium Concentration (ppb Se)	Percent Se as Selenite *	Resin Form	Resin Wet Weight (g)	Percent Removed
452	100	Fe^{+++}	0.77	90
697	55	Fe^{+++}	0.75	53
697	55	Ba^{++}	0.71	19
697	55	Fe^{+++},Ba^{++}	0.55 (Fe), 0.65 (Ba)	47

*Balance as selenate

All experiments used resin plus 100 ml of solution containing 176 ppm sulfate, 30 ppm chloride and 104 ppm sodium in addition to the selenium.

The next step was to apply these results to a column study. Twenty-five milliliters of Duolite C-464 weak-acid cation exchanger (in the ferric form) was loaded into a half-inch diameter column and fed a solution containing 50 ppm chloride, 260 ppm sulfate, and 997 ppb selenium (as selenite) at a flowrate of 1.84 gal/(min ft^2). Sodium was the only cation. The effluent-concentration history, shown in Figure 13, indicates that sixteen bed volumes of feed were processed before selenium broke through at a concentration of 10 ppb.

While the capacity of this particular run is lower than that for ion exchange under similar circumstances, the run does indicate that the process is feasible and that a selenite-selective material can be produced. Improvements to this idea are likely in future investigations.

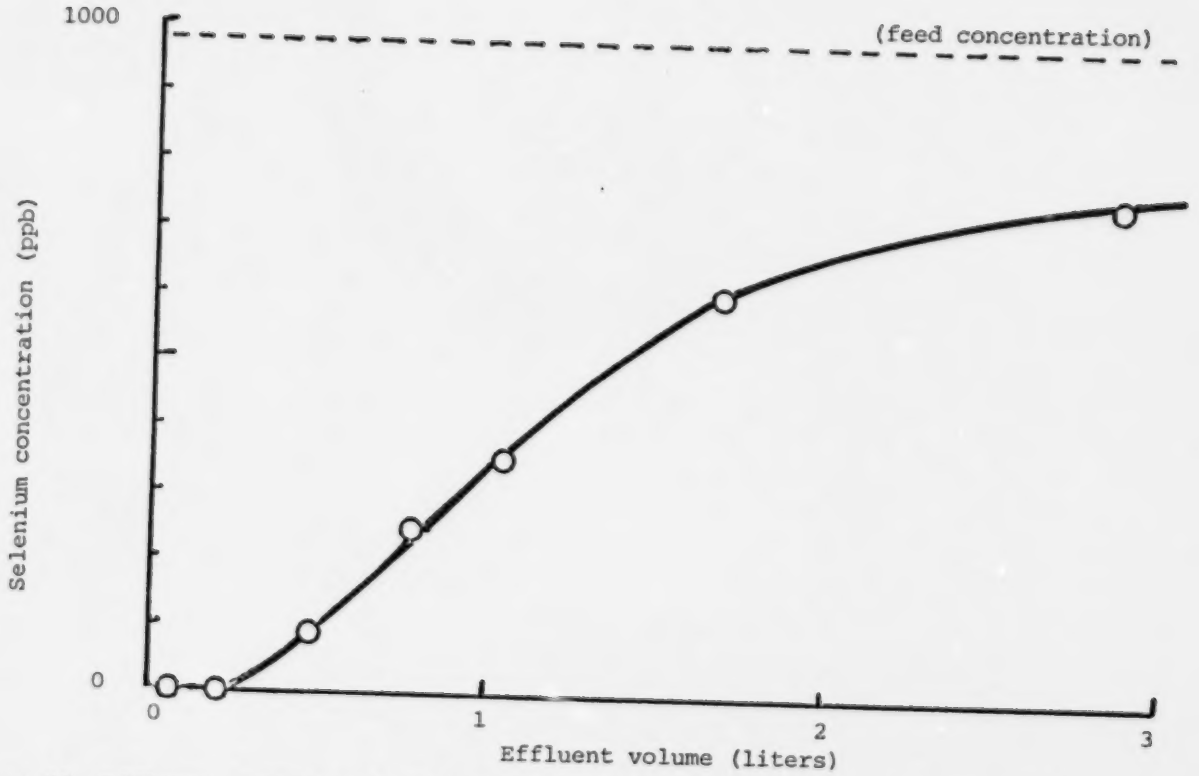

Figure 13. Effluent-concentration history for removal of selenite by weak-acid ion-exchange resin Duolite C-464 in ferric form. 997 ppb Se, 260 ppm $SO_4^=$ and 50 ppm Cl^- in feed.

SECTION 5

DESIGN EXAMPLE

The use of ion exchange for selenium removal is illustrated here by an example that utilizes the information presented in Section 3. Some of the key ideas are first re-summarized for convienence.

1) Selenite and selenate in drinking water are normally present in trace concentrations. The trace-principle concept developed in Appendix A1 may thus be applied to simplify performance prediction.

2) Selenate is virtually identical to sulfate in its ion-exchange behavior. Hence, under given feed and bed presaturation compositions, the capacity of a bed for selenate removal can be inferred from its capacity for sulfate removal.

3) Selenite is slightly less preferred than nitrate for the resin studied (Dowex 2X8) so that selenite-removal capacities can be estimated from those for nitrate.

The composition of drinking water varies from one location to another so that to define an "average" drinking water has little meaning. The predominant ionic species are usually the same, however. Sulfate, chloride and bicarbonate compose the bulk of the anionic composition with nitrate and other ions (such as phosphate) present in smaller amounts. In the example presented in this section, the water will be assumed to contain sulfate, chloride and nitrate in addition to the trace selenium species (cf. Table 8).

TABLE 8. REPRESENTATIVE WATER COMPOSITION FOR TEXT EXAMPLE

Ion	Concentration		Equivalent Fraction (x^o)
	ppm	normality	
Sulfate	120	0.00250	0.5000
Chloride	80	0.00225	0.4495
Nitrate	15.5	0.00025	0.0500
Selenate	50 ppb Se	1.25×10^{-6}	0.00025
Selenite	50 ppb Se	1.25×10^{-6}	0.00025
		0.0050	1.0000

Even though bicarbonate can often make up a considerable fraction of the total dissolved solids in water, it has been ignored because of its position in the selectivity sequence (Table 3). It is the least preferred species so that its effect on selenate or selenite removal will be small. Nitrate, while normally at concentrations lower than those of bicarbonate, is included in the water to be studied, again because of its position in the selectivity sequence of Table 3. The preference of the exchanger for nitrate is intermediate with respect to the selenium species so that nitrate concentrations, even at levels below the maximum contaminent level of 10 mg/L NO_3^-–N, can reduce selenite-removal capacities (see Figure 11).

The following procedure will provide a quick estimate of the performance of strong-base resins (as represented by Dowex 2X8) for removing selenium. The entire method is based on the premises of the local-equilibrium theory. As noted in Basic Concepts for Fixed-Bed Analysis in

Section 3, these assumptions give qualitatively correct results that should suffice for initial process design. Additionally, the resin bed is assumed to be in the chloride form initially.

1) Treat the sum of the bicarbonate and chloride equivalent fractions ($x^{\circ}_{HCO_3}$ and x°_{Cl}) as an effective chloride fraction ($x_{Cl}' = x^{\circ}_{HCO_3} + x^{\circ}_{Cl}$).

2) From the composition of the water to be treated, and a given set of separation factors (such as those in Table 3), calculate the equivalent fraction of sulfate in the resin phase from the relation,

$$y^{\circ}_{SO_4} = \frac{x^{\circ}_{SO_4}}{x^{\circ}_{SO_4} + \alpha_{SO_4,NO_3}\, x^{\circ}_{NO_3} + \alpha_{SO_4,Cl}\, x_{Cl}'} \qquad (16)$$

(see Appendix A1, Eq. A1.2).

3) Compute the ratio of the resin-phase equivalent fraction to the fluid-phase equivalent fraction for sulfate at the feed composition ($y^{\circ}_{SO_4} / x^{\circ}_{SO_4}$). As shown in Appendix A1, this ratio gives the breakthrough T value at which the sulfate fraction saturates the bed (T_{SO_4}). Because the exchanger does not distinguish between selenate and sulfate, this is also the T-value at which selenate breaks through the bed (T_{SeO_4}).

4) Determine the capacity for selenate by converting T_{SeO_4} to bed volumes of feed with Eq. 14.

5) Use the feed composition, along with Fig. 11, to determine the capacity for selenite in terms of bed volumes of feed.

This method will under-predict breakthroughs of the selenium species when the equivalent fraction of bicarbonate in the feed is high. The estimates made here are thus conservative.

For the feed composition shown in Table 8, $y^{\circ}_{SO_4}$ is found to be 0.988, so that $T_{SeO_4} = y^{\circ}_{SO_4} / x^{\circ}_{SO_4} = 1.98$. From Eq. 13, this corresponds to a capacity for selenate of 515 bed volumes of feed (for Dowex 2X8, $\rho_b Q$ = 1.3 meq/ml and ϵ = 0.4). Figure 11 shows that for the given feed composition, the capacity for selenite is 442 bed volumes of feed.

Note the effects of nitrate and sulfate on selenium removal in this example. If no nitrate were present ($x^{\circ}_{NO_3}$ = 0), and for constant total concentration (increased x°_{Cl} makes up for the absence of nitrate), the removal of selenate and selenite would be the same, each with a capacity of 494 bed volumes of feed. Because the four-component sulfate-chloride-selenate-selenite system can be treated as the two-component sulfate-chloride system (due to the trace levels of the selenium species), selenite, being favored less by the resin than sulfate but more than chloride, will emerge from the bed just ahead of the sulfate fraction. Selenate is identical to sulfate and will emerge when sulfate does. So, even when the concentration of nitrate is below its maximum concentration limit ($x^{\circ}_{NO_3}$ = 0.143 under the conditions of Table 8), it has a significant effect on the removal of selenite.

If no sulfate were present, and the fraction of chloride correspondingly increased, the removal capacity for selenate would be 4030 bed volumes (see Eq. 16 with $x^{\circ}_{SeO_4}$ substituted for $x^{\circ}_{SO_4}$). The capacity for selenite would be 1040 bed volumes (Figure 11). Note the large expected increases in the capacities over the case where sulfate is present. In this situation, each ion breaks through the bed at its trace capacity.

APPENDIX A1

Equilibrium and Fixed-Bed Theory

This appendix contains general considerations on ion-exchange equilibrium and on local-equilibrium theory of ion exchange columns.

1. Constant-Separation-Factor Model

For a binary system, y_i (i = 1 or 2) is an explicit function of the corresponding x_i found, by combining Eqs. 4, 5 and 7 in the text.

$$y_1 = \frac{\alpha_{12} x_1}{1-(\alpha_{12}-1)x_1} \tag{A1a}$$

$$y_2 = \frac{\alpha_{21} x_2}{1-(\alpha_{21}-1)x_2} \tag{A1b}$$

For a ternary (three-component) system, the corresponding expresions are,

$$y_1 = \frac{x_1}{x_1 + \alpha_{21} x_2 + \alpha_{31} x_3} \tag{A2a}$$

$$y_2 = \frac{x_2}{\alpha_{12} x_1 + x_2 + \alpha_{32} x_3} \tag{A2b}$$

$$y_3 = \frac{x_3}{\alpha_{13} x_1 + \alpha_{23} x_2 + x_3} \tag{A2c}$$

Here, y_i is not solely a function of x_i.

For systems with three or more components, the general relation

$$y_i = \frac{x_i}{\sum_{j=1}^{n} \alpha_{ji} x_j} \tag{A3}$$

may be used to calculate a set of resin-phase fractions from a given set of fluid-phase fractions. Given a set of y_i, the corresponding x_i can be found from

$$x_i = \frac{y_i}{\sum_{j=1}^{n} \alpha_{ij}\, y_j} \qquad \text{(A4)}$$

A discussion of other equilibrium models and relations can be found in Reference 33.

2. Effluent Concentration Histories and Axial Concentration Profiles

An effluent concentration history (ECH) is a record of the variation in the composition of the effluent from an ion exchange column, such as shown in Figures 1, 4, 12, and A6 through A9 (Appendix A5). For discussions to follow, an ECH will be defined as the set of functions, x_i (T), the x_i being measures of composition, and T, the measure of effluent volume at constant bed volume.

An axial concentration profile (CP) is a record of the resin composition along the bed axis at a given time. A CP will be defined as the set of functions, y_i (1 / T), the y_i being measures of composition and 1/T, a measure of the distance along a bed for a given feed volume (cf. Eq. 12 in the text).

Within the local equilibrium theory, the ECH and the CP represent the same phenomenon from two points of view. An ECH sets a bed volume, v, and records the change in the effluent composition with effluent volume V. A CP, on the other hand, sets a feed volume and records the change in resin-phase composition with the distance along the bed axis.

The major features of an ECH or CP are transitions (T-values or T-intervals for which composition is changing) and plateaus (T-values or T-intervals for which composition is constant). For the practically important case of an n-component feed passing through a bed uniformly presaturated with one of the components, the ECH or CP usually comprises n-1 transitions and n plateaus. Exceptions to this have been discussed by Helfferich and Klein (15).

Transitions can be divided into two categories:

Abrupt Transitions - Under the premises of the local-equilibrium, this type of transition occurs when the equilibrium isotherm is favorable for uptake of a feed component over the presaturating species. Abrupt transitions are mathematical discontinuities in the ECH or CP because all concentrations change at a single value of T. In real systems, rate effects replace the discontinuity with a smooth, sigmoid curve (compare Figures 1 and 4 in the text).

Rate effects do not continue to spread these transitions over larger intervals of T. Rather, as the transition moves through the bed, it tends assume a constant form resulting from a balance between the dispersive rate processes and the sharpening effects of a favorable isotherm. This is termed constant-pattern behavior and is shown in Figure A1a.

Gradual Transitions - This type of transition occurs if the equilibrium isotherm is unfavorable for uptake of a feed component over the presaturating species. In real or equilibrium systems, this type of transition spreads as it moves through the bed of resin because the leading edge of the transition moves faster than the trailing edge. This is termed proportionate-pattern behavior. An CP for a proportionate-pattern transition (at two times) as it moves through a bed of resin is shown in Figure A1b.

Exhaustion operations normally involve equilibrium-favored transitions because proportionate-pattern transitions do not utilize the bed of resin as efficiently as do constant-pattern transition (compare Figure A1a and A1b). However, proportionate pattern transitions sometimes cannot be avoided during regeneration (see, for example, Figure 12 in the text).

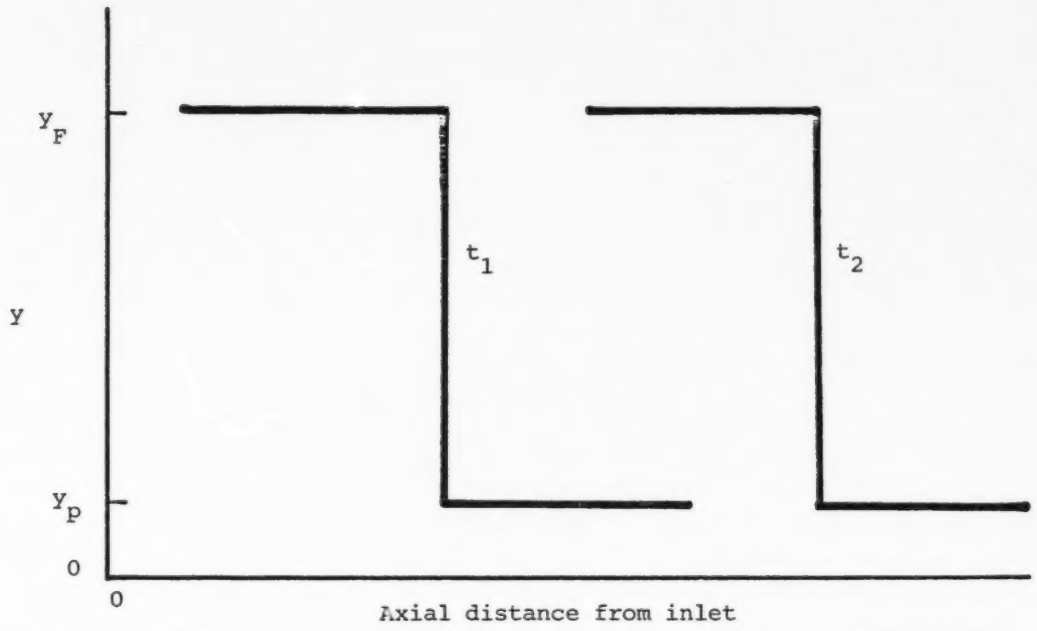

Figure A1a. Movement of abrupt transition (shown at times t_1 and $t_2 > t_1$) under premise of local equilibrium.

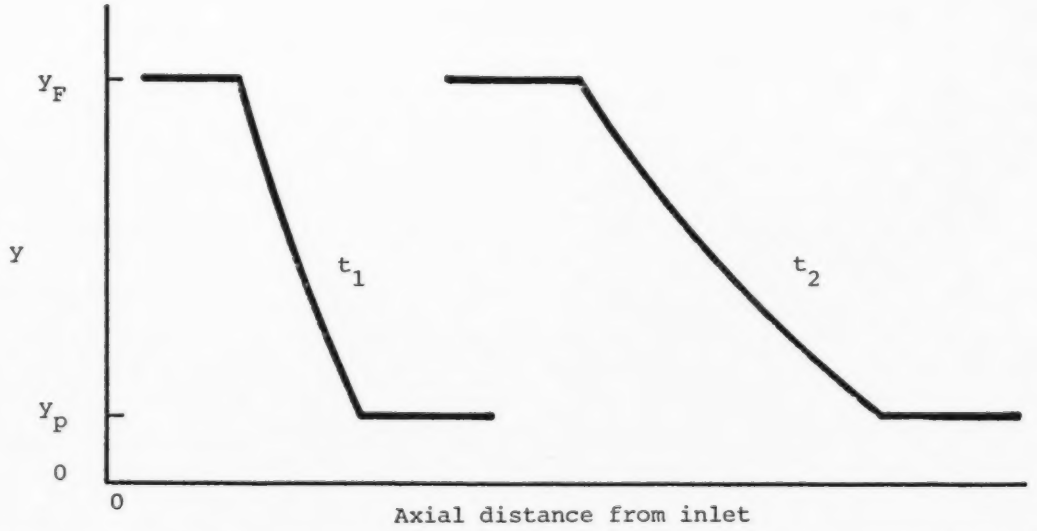

Figure A1b. Movement of gradual transition (shown at times t_1 and $t_2 > t_1$) under premise of local equilibrium.

A transition can be thought of as a wave across which compositions change. By analogy then, with each transition, there is associated a spectrum of velocities with which the wave moves through a bed of resin. For example, Figure 4 in the text shows this for a three-component system. The two waves (abrupt transitions) in this case, move at different velocities so that they reach the bed outlet at a different times. Hence, two distinct transitions are observed.

The prediction of an ECH or CP requires solution of a set of material-balance equations (see References 15, 20 and 33). The solution involves an eigenvalue problem, in which the wave velocities mentioned above arise as the eigenvalues. This approach is fully discused by Helfferich and Klein (15) and Rhee, et.al. (20). The next sections will cover the more pertinent details of their work.

3. Prediction of Fixed-Bed Performance

The equations necessary to predict the performance of a fixed bed under the premise of the local equilibrium are presented below. In all cases, the bed is assumed to be uniformly presaturated and to recieve a feed of constant composition.

3.1. Binary systems

For a two-component system, there is one transition that joins two plateaus. The composition of the feed plateau (x_{i_F} or y_{i_F}) and the presaturation plateau (x_{i_P} or y_{i_P}) can be used to determine the range of T-values for a transition through a material balance. For abrupt transitions ($\alpha_{ij} > 1$) the T-value, T_Δ, for which the feed concentration of Component i appears in the effluent is given by (33),

$$T_\Delta = \frac{\Delta y_i}{\Delta x_i} = \frac{y_{i_F} - y_{i_P}}{x_{i_F} - x_{i_P}} \tag{A5}$$

where Δ signifies the composition change between the plateaus. If Component i is absent from the bed initially, $y_{i_P} = x_{i_P} = 0$ and the transition T-value is given by,

$$T_\Delta = \frac{y_{i_F}}{x_{i_F}} \tag{A6}$$

For gradual transitions, it can be shown (33) that T is a function of x_i is given by

$$T = \frac{dy_i}{dx_i} = \frac{\alpha_{ij}}{[1 + (\alpha_{ij} - 1)x_i]^2} \tag{A7}$$

if the constant-separation-factor model is used. The T value for the leading edge of the transition is found by using the presaturation composition ($x_i = x_{i_P}$). The T value for the trailing edge is found by using the feed composition. ($x_i = x_{i_F}$). Intermediate T values intermediate are obtained by using intermediate x_i values.

3.2. Ternary systems

The ECH or CP for a ternary system comprises three plateaus and two transitions. Figures 1 and 4 in the text are examples of such a history. To predict a history or profile satisfactorily, the composition of all plateaus and the T-values over which the transitions occur must be determined. The following discussion will treat only histories or profiles with abrupt transitions. The same principles apply to the prediction of gradual transitions but the computations are more involved. A complete review of calculation methods for ternary systems can be found in References 15, 20 and 33.

The behavior of a 3-component system can be considered as a prototype for the behavior of more complex multicomponent systems. While the computations for ternary systems are more complex than those for binary systems, the ternary system is a true multicomponent system that has a manageable analytical solution to the material-balance problem (see above, Effluent Concentration Histories and Axial Concentration Profiles).

The only feature of a binary ECH or CP with an abrupt transition that had to be determined is the position of the transition in terms of T since the compositions of the plateaus involved were set by boundary conditions (i.e., the feed and presaturation compositions). In contrast, for a three-component system with abrupt transitions, there are three unknown features; the position of two transitions and the composition of a plateau that separates them. As before, the feed and presaturation plateau compositions are set by the boundary conditions. A rigorous mathematical approach may be used to find these quantities (20). In this section, a simple graphical method, equivalent to the rigorous mathematical method, is discussed (15). The graphical technique shows clearly the process by which the unknown quantities in an ECH or CP are determined.

To streamline the discussion, the following nomenclature will be used:

Plateaus: The plateaus in a three-component ECH or CP will be identified as:

1) Feed plateau - The composition of this plateau is specified by the given feed composition.

2) Middle plateau - The composition of this plateau is to be determined as a result of the analysis.

3) Presaturation plateau - The composition of this plateau is specified by the given bed presaturation composition (taken to be uniform).

Transitions: The abrupt transitions in a three-component ECH or CP will be identified by their T-values as:

1) T_1 - This transition separates the feed and middle plateaus.

2) T_2 - This transition separates the middle and presaturation plateaus.

The graphical approach uses the triangular composition diagram, an example of which is shown in Figure A2. In such diagrams, the sum of the perpendicular distances from an internal point inside the diagram to the sides of the diagram is a constant. Taking this constant to be unity makes the distances equal to the equivalent fractions, x_i or y_i (see Eqs. 4 and 5 in the text). Thus, each point in the diagram represents a set of compositions in the fluid- or resin-phase that can be used to determine the composition of the other phase (see Eqs. A3 and A4). Along the sides of the diagram, the fraction of one component is zero. Thus, each edge represents one of the binary systems that can be created from three components (the 1-2, 2-3 and 1-3 binaries). At each vertex, one of the components is present in pure form.

The local-equilibrium analysis of a ternary system may be carried out simply on a triangular diagram. On this diagram, plateaus appear as single points (such as F, MP, MP' and P in Figure A2) while transitions appear as curves (such as curves F-MP and MP-P in Figure A2). The diagram can be considered as a topographic map of an ECH or CP if T is considered as the third dimension, perpendicular to the plane of the diagram. If constructed with y_i as the coordinates, the diagram will produce an axial concentration profile. If the coordinates are x_i, the diagram will show an effluent concentration history. Further discussions on the construction and use of the triangular diagram may be found in Reference 15.

Prediction of a three-component ECH or CP starts with the given boundary conditions of the feed and presaturation plateaus (points F and P, respectively in Figure A2). The result needed is the sequence of compositions (termed the composition route) that connects these two points. To calculate the ECH or CP, this route is then translated to a T-scale.

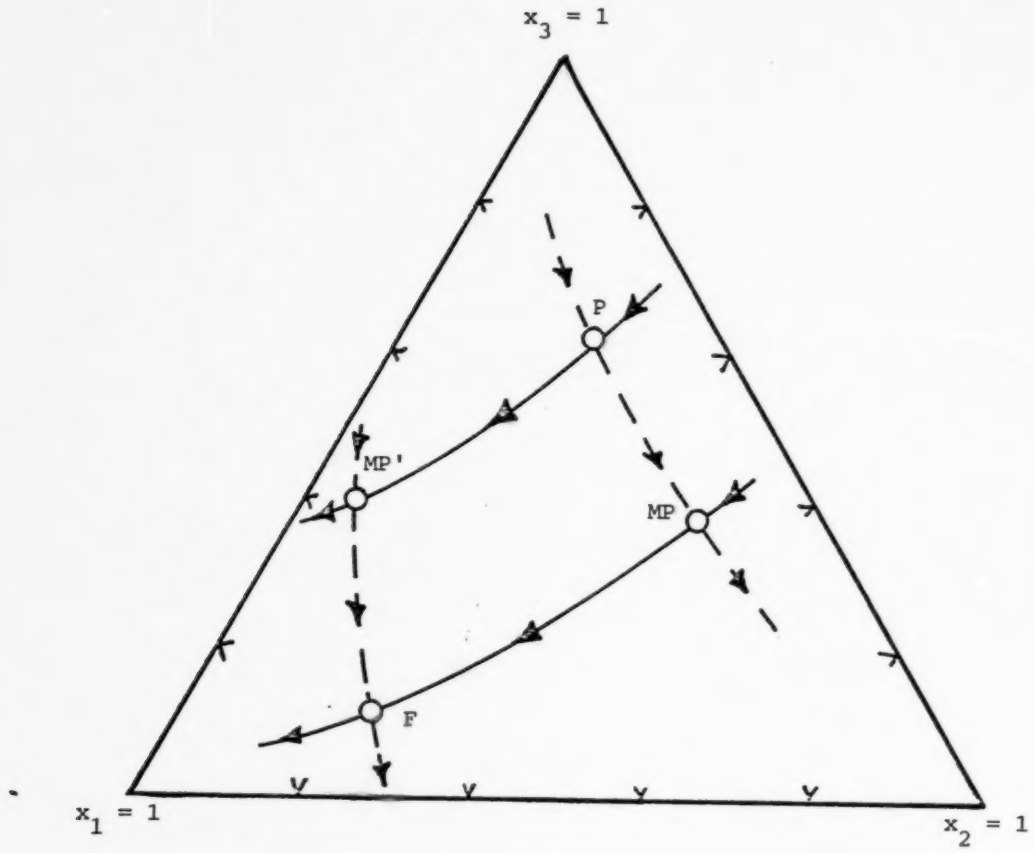

Figure A2. Composition-path diagram on basic x-grid for ternary system. Solid lines, Type-1 paths; Dashed lines, Type-2 paths. Feed (F), Middle (MP) and Presaturation (P) plateaus shown.

While an infinite number of curves can be used to connect points F and P, there are only certain allowable "paths" (which result from the solution of the eigenvalue problem) that can be followed in going from point F to point P. These composition paths are fixed by the governing equilibrium isotherms (such as Eqs. 6 in the text) and a representative grid of such paths can be constructed on the diagram. In general, n-1 composition paths will pass through each "point" in the n-dimensional composition space for an n-component system. Accordingly, a three-component system has two paths through every point in the triangular diagram. This is illustrated in Figure A2 where the two paths are drawn through the given feed and plateau points (in accordance with the guidelines of Reference 15 but not based on a particular isotherm model). The composition route representing the ECH or CP can only follow along such paths. For the particular case of the constant-separation-factor model, the composition paths can be shown to be straight lines. Figure A4 is an example of such a system.

The two types of paths shown in Figure A2 will be designated Type 1 (solid lines) and Type 2 (dashed lines). An important property of composition paths is that paths of the same type do not intersect each other inside the diagram. This means that the composition route must switch paths if the feed and presaturation points do not happen to lie on the same composition path. For example, in Figure A2, point F and P do not lie on the same path and the composition route jumps from one path to another (such as through the routes F-MP-P or F-MP'-P). The arrows on the paths indicate the direction in which the velocities of compositions along the path increase.

The following rules will specify the exact route taken from the feed point (F) to the presaturation point (P).

1) The composition route starts from point F only on a Type 1 path

2) At the point where the Type 1 path from F intersects a Type 2 path passing through P, the route jumps to the Type 2 path to reach point P.

The procedure shows that the correct route in Figure A2 is the F-MP-P route.

The point at which the route jumps from a Type 1 path to a Type 2 path represents the composition of the middle plateau. Since the route from F to P has been identified, the transitions for the system have also been determined. The following rules will determine the transition types from the diagram:

1) A transition is **abrupt** if the dirtection of the composition route is opposite to the direction of the arrows on the composition path. Route F-MP-P, for example, has two abrupt transitions.

2) A transition is **gradual** if the direction of the composition route is in the direction of the arrows on a composition path. If the route F-MP'-P were followed, the two transition would be gradual.

Thus, the graphical method directly gives the necessary information for a ternary system ECH.

The T-values at which the abrupt transitions occur can be calculated from Eq. A5 in the form,

$$T_1 = \frac{y_{iF} - y_{iMP}}{x_{iF} - x_{iMP}} \tag{A8}$$

$$T_2 = \frac{y_{iMP} - y_{iP}}{x_{iMP} - x_{iP}} \tag{A9}$$

The subscripts F, MP and P represent respectively, the feed, middle and presaturation plateau compositions. Calculation methods for gradual transitions may be found in References 15 and 33.

3.3. Higher-order Systems

The so-called H-function, has been developed to deal with multicomponent systems described by the constant-separation-factor model (15). This technique transforms compositions (either resin- or fluid-phase) to values of a single variable, "h". This variable has several desireable and simple properties that allow it to solve quite complex problems. When a problem is solved in terms of the h, it is a simple step to recover the answer in terms of the concentration variables. For systems of more than three components, numerical methods are required. A computer program that uses the H-function for problems involving up to 11 exchangeable species under general boundary conditions has been developed (34).

4. Trace Behavior

When one species is present in concentrations that are low relative to the others in a mixture, it is termed a trace species. The non-trace species are termed gross species. In systems where all but one component (taken to be the most weakly held component) are present as traces, the behavior is simplified because the gross component supresses interference between the traces. A multicomponent system can then be treated as a set of trace-gross binary systems. In constant-separation-factor systems, the local-equilibrium theory predicts that the T-value for each of the (abrupt) transitions to be,

$$T_i = \alpha_{i\,gross} \tag{A10}$$

where T_i is the value of T at which the concentration of Component i rises to its feed concentration. This behavior is found in frontal-analysis chromatography where an inert carrier (the gross component) is used to separate a mixture into its component species. If there is more than one gross component, more complicted phenomena can arise (see Appendix A3). A complete discussion of this topic can be found in Reference 15.

APPENDIX A2

Discussion of Figures 9 and 10

This Appendix discusses Figures 9 and 10 in the text. The behavior of the sulfate-chloride-selenate system at several total concentrations is examined with the objective of determining the effects of sulfate concentration on the removal of selenate. The effects of nitrate and bicarbonate ions are not considered as their presence will have little to no effect on selenate removal when sulfate is present. This is due to the high selectivity of the resin for selenate and sulfate over nitrate and bicarbonate. Chloride is included for its role as presaturating ion.

In Figure 9, the selenate-chloride isotherm is used to determine graphically the breakthrough T value for any given influent concentration of selenate ($x^{\circ}_{SeO_4}$) for the selenate-chloride system. If no selenate is on the bed initially, the breakthrough T-value can be determined from the relation (see Appendix A1, Eq. A6)

$$T^{*} = \frac{y^{*}_{SeO_4}}{x^{\circ}_{SeO_4}} \tag{A11}$$

where $y^{*}_{SeO_4}$ is the resin-phase equivalent fraction of selenate in equilibrium with the feed composition. From this equation, it is possible to interpret T^{*} as the slope of the line on an x-y plot that connects the point ($y^{*}_{SeO_4}$, $x^{\circ}_{SeO_4}$) on the isotherm, with the origin. The breakthrough T-value (T^{*}) may be found by extending the line connecting the origin and this point to the T axis. This procedure does not require an analytic expression for the isotherm and is therefore applicable to a favorable isotherm of arbitrary shape.

Figure 10 shows the effects of sulfate on the removal of selenate. In the Figure, the capacity for selenate (in terms of bed volumes of feed) is plotted against the ratio of sulfate and selenate fractions in the feed (γ). Since sulfate and selenate were found to be identical, the effect can be seen directly from Figure 9, with $x^{\circ}_{SeO_4}$ replaced by $x^{\circ} = x^{\circ}_{SeO_4} + x^{\circ}_{SO_4}$. Here, x° is the combined fraction of selenate and sulfate in the feed and can be considered as an effective selenate fraction. As the sufate fraction in the feed increases relative to the selenate fraction, x° increases and the value of T at which the combined sulfate-selenate fraction breaks through the bed (T^{*}) approaches unity. This calculation has been repeated for several total concentrations, using the following expressions:

Effective selenate fraction,

$$x^{\circ} = x^{\circ}_{SeO_4} + x^{\circ}_{SO_4} \tag{A12}$$

Sulfate-to-selenate ratio,

$$\gamma = \frac{x^{\circ}_{SO_4}}{x^{\circ}_{SeO_4}} \tag{A13}$$

Effective selenate fraction in terms of the selenate fraction and γ,

$$x^{\circ} = x^{\circ}_{SeO_4}(1 + \gamma) \tag{A14}$$

Dependence of the separation factor on the total concentration.

$$\alpha_{SeO_4,Cl} = \alpha = 0.2\, C_o^{-0.85} \tag{A15}$$

Resin-phase fraction for the combined selenate-sulfate fraction.

$$y^* = \frac{\alpha x^\circ}{1 + (\alpha - 1)x^\circ} \tag{A16}$$

The resin-phase fraction in terms of the selenate fraction and γ.

$$y^*(\gamma) = \frac{\alpha x^\circ_{SeO_4}(\gamma + 1)}{1 + (\alpha - 1)(\gamma + 1)x^\circ_{SeO_4}} \tag{A17}$$

Breakthrough T-value for the combined selenate-sulfate fraction.

$$T = \frac{y^*(\gamma)}{x^\circ} \tag{A18}$$

Capacity at breakthrough, in terms of bed volumes of feed.

$$\frac{V}{v} = \frac{\rho_b Q}{C_o} T + \epsilon \tag{A19}$$

Equations A18 and A19 were used to directly construct Figure 10 for a selenate feed concentration of 50 ppb selenium. For Dowex 2X8, $\rho_b Q$ is 1.3 meq/ml. The expression in Eq. A15 was determined from the data in Figure 5 in the text.

As an example, the capacity prediction for the first exhaustion run (see Table 4) will be carried out. From the given concentrations, the total solution concentration was found to be 0.0054 N. The selenate and sulfate feed fractions ($x^\circ_{SeO_4}$ and $x^\circ_{SO_4}$) are then 0.0000012 and 0.742, respectively.

$$x^\circ = 0.742$$

$$\gamma = 620{,}000$$

$$\alpha_{SeO_4,Cl} = \alpha = 16.95$$

$$y^* = 0.980$$

$$T = 1.32$$

$$\frac{V}{v} = 320$$

APPENDIX A3

Discussion of Figure 11

This appendix discusses the removal of trace amounts of selenite from waters containing nitrate, sulfate and chloride. It is the background for the construction of Figure 11 in the text. In all cases examined, feeds containing these ions, at a total concentration of 0.005 N are fed to a column uniformly presaturated with chloride. The relevant separation factors are those given in Table 3 of the text.

Case 1: Water contains nitrate and chloride but not sulfate.

As shown in the discussion of the trace-component principle (Appendix A1), when nitrate and selenite are both present in minute econcentrations, the breakthrough T-values for each ion may be determined from their respective separation factor values relative to chloride. Thus,

$$T_{SeO_3} = \alpha_{SeO_3 \cdot Cl} \tag{A20a}$$

$$T_{NO_3} = \alpha_{NO_3 \cdot Cl} \tag{A20b}$$

If the nitrate fraction in the feed is increased (at the expense of the chloride fraction), nitrate will break through at a T-value lower than that predicted by Eq. A20b. Examples are shown in Figure A3.

In Figure A3a, nitrate and selenite are present as traces. The breakthrough T-values for this case are given by Eqs. A20. Higher nitrate levels in the feed cause the nitrate breakthrough to drop below $\alpha_{NO_3 \cdot Cl}$. However, since selenite breaks through in the presence of chloride alone, it still does so at $\alpha_{SeO_3 \cdot Cl}$. This is shown qualitatively in Figure A3b. Eventually, a nitrate feed level is reached such that T_{NO_3} becomes smaller than $\alpha_{SeO_3 \cdot Cl}$ (Figure A3c). In this case, the nitrate breakthrough "chases" the selenite breakthrough out of the column before the expected $T = \alpha_{SeO_3 \cdot Cl}$. Therefore, even though the selenite feed concentration is unchanged, higher nitrate feed concentrations reduce the capacity of a bed for selenite. Also, the Figure shows that a spike of selenite will precede the nitrate breakthrough. The low concentration of selenite means that the width of the spike will be very small so that the selenite breakthrough can be estimated from the nitrate breakthrough ($T_{SeO_3} \approx T_{NO_3}$).

In Figure 11, the curve for $x_{SO_4} = 0$ was generated with the above ideas in mind. Since the selenite fraction is small ($x_{SeO_3} = 0.0005$), it can be ignored and the ternary system of selenite, nitrate and chloride can be treated as the binary system of nitrate and chloride. The point at which nitrate breakthrough would begin to interfere with selenite breakthrough can be found by determining the nitrate fraction at which the breakthrough T value is equal to that of selenite (i.e., $T_{NO_3} = \alpha_{SeO_3 \cdot Cl}$). At higher fractions of nitrate, selenite breakthrough can be estimated from that of nitrate.

Case 2: Water contains sulfate and chloride but no nitrate

This situation is analogous to Case 1, with sulfate replacing nitrate. The difference in this case is the relative selectivity of the resin for sulfate over nitrate. The same effects will be observed, however.

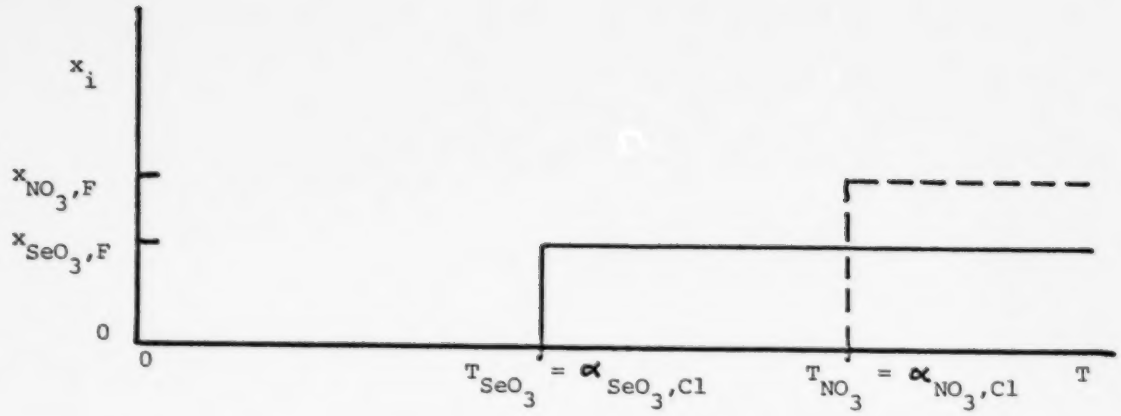

a) Breakthrough when each ion is present as a trace

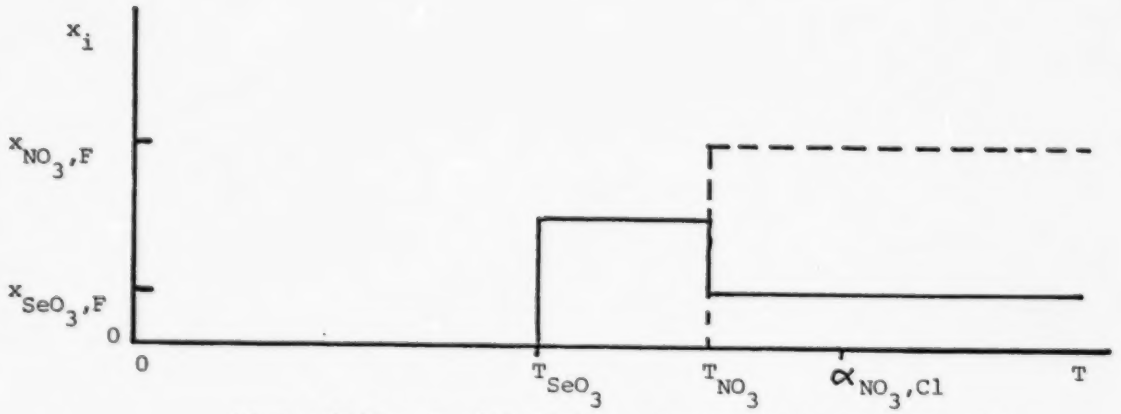

b) Breakthrough with higher nitrate feed level but with selenite still as a trace

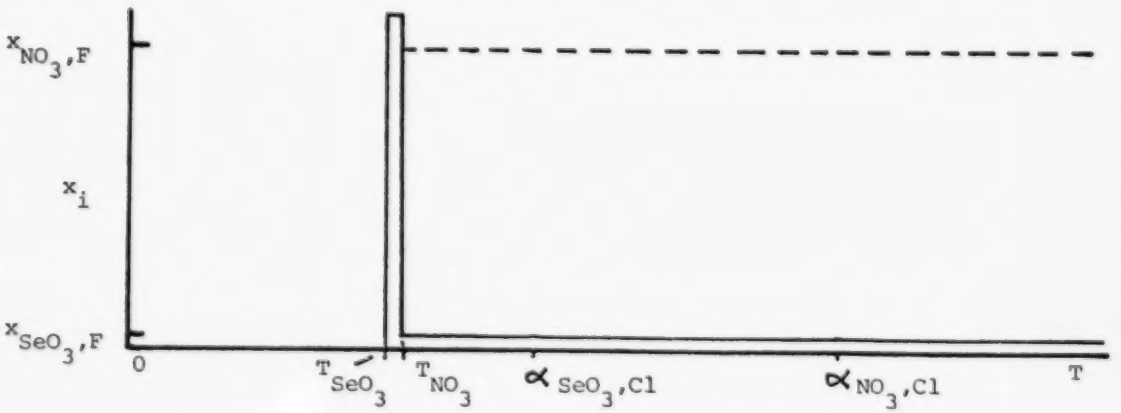

c) Breakthrough at high nitrate concentration with selenite as a trace

Figure A3. Effect of nitrate on selenite removal (schematic).

Case 3: Water contains sulfate, nitrate and chloride

In this four-component system, the selenite fraction is small enough to be ignored so that the mixture can be treated as the ternary system of sulfate, nitrate and chloride. The breakthrough of selenite is estimated from that of nitrate. The technique used here is based on the triangular composition path diagram shown in Figure A4 (see Appendix A1 for a discussion of such diagrams). The following procedure was followed to generate the curves in Figure 11:

1) Choose a sulfate feed fraction ($x^{\circ}_{SO_4}$)

2) Choose a nitrate fraction such that $x^{\circ}_{SO_4} + x^{\circ}_{NO_3} + x^{\circ}_{Cl} = 1$. This sets the feed point, F, in Figure A4.

3) Using Figure A4, determine the midplateau (Point MP on the Figure) composition associated with the feed composition $x_{NO_{3MP}}$ and $y_{NO_{3MP}}$.

4) The presaturation composition (Point P in Figure A4) contains only chloride ($x_{NO_{3P}} = y_{NO_{3P}} = 0$). This means that the nitrate transition is given by the ratio of the nitrate resin-phase fraction to the nitrate fluid-phase fraction at the mid-plateau composition (Eq. A9).

This procedure determines the T-value for the nitrate breakthrough (T_{NO_3}). As long as this is smaller than $\alpha_{SeO_3,Cl}$, this is also the selenite breakthrough. When T_{NO_3} is greater than $\alpha_{SeO_3,Cl}$, the selenite breakthrough remains at $T_{SeO_3} = \alpha_{SeO_3,Cl}$. Eqs. 13 and 14 in the text can be used to convert this to capacity in terms of bed volumes of feed.

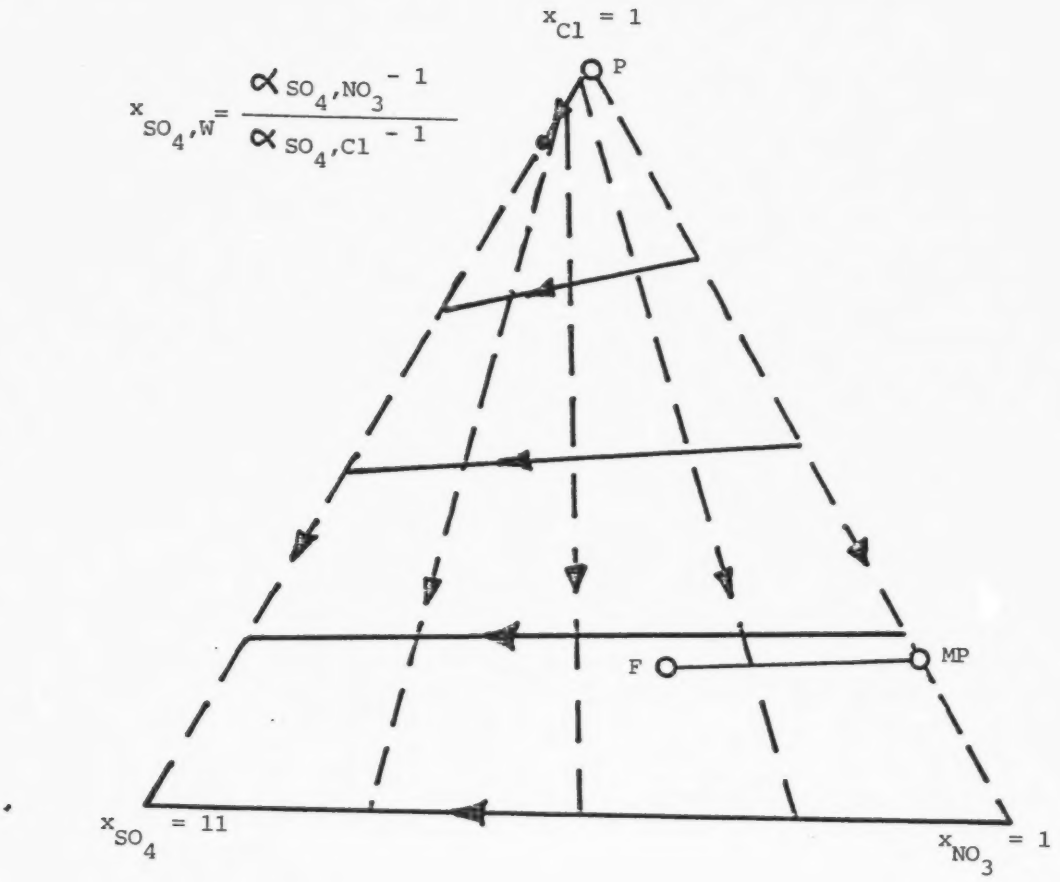

Figure A4. Composition-path diagram for sulfate-nitrate-chloride system at 0.005 N. $\alpha_{SO_4,Cl} = 20$, $\alpha_{SO_4,NO_3} = 3$. x_w point is the watershed point (see References 15 and 33). Example of composition route: F-MP-P.

APPENDIX A4

Experimental Methods for Generating Isotherms

1. Batch method

This technique uses a batch contacting scheme. It produces a set of equilibrium-related fluid- and solid-phase concentration data that may be used to determine the parameters of an equilibrium model for a binary system. The procedure was as follows:

1) Convert the resin fully to one ionic form. Of the pair of ions being examined, one has an initial resin-phase equivalent fraction of unity ($y_i^\circ = 1$) while the other, a fraction of zero.

2) Accurately weigh a portion of this resin (say m grams) and place in a flask. Given the dry weight exchange capacity (Q') and the moisture content of the resin (w grams water/gram dry resin), the total number of resin equivalents for the experiment is fixed as mQ ($= mQ'/w$).

3) Add a solution of known concentration (C_o), composition (x_i°) and volume (V).

4) Allow sufficient time for equilibration.

5) When the system has equilibrated, the composition of the liquid phase is determined giving the equilibrium fluid-phase fractions of the components (x_i^*).

The material balance for exchangable Ionic Species i takes the form:

Equivalents of Species i present initially = Equivalents of Species i at equilibrium

or, in terms of experimental quantities,

$$x_i^\circ C_o V + y_i^\circ mQ = x_i^* C_o V + y_i^* mQ \tag{A21}$$

Solving for the only unknown, y_i^*, gives,

$$y_i^* = y_i^\circ + \frac{C_o V}{mQ}(x_i^\circ - x_i^*) \tag{A22}$$

For each repetition of the procedure, a set of x_i^* and y_i^* values is generated. This method was used to produce Figures 5 through 8 in the text.

2. Column Method

This method utilizes the effluent concentration history of a column run in conjunction with an equivalent balance to produce a single point on the isotherm. For a binary system, the following procedure was used:

1) Convert a bed of resin fully to one ionic form by passing a solution of the ion through the bed.

2) Prepare a feed solution containing the two ions to be studied. The solution is of known total concentration (C_o) and composition (x_i°).

3) Pass the feed through the resin bed and collect all of the effluent in a single container. As the operation progresses, periodically check the fluid phase composition of the effluent coming directly from the column. When the composition of the effluent matches that of the feed, stop the operation.

4) Record the total volume (V') and the average composition of the effluent collected ($\bar{x}_i$).

A material balance on Ionic Species i takes the form,

Input - Output = Accumulation in the column

With the basis of one equivalent of resin in the column, this becomes,

$$x_i^o T' - \int_0^{T'} x_i(T)\, d\, T = y_i^* \tag{A23}$$

where $x_i(T)$ is the effluent-concentration history of component i. T' corresponds to the volume of effluent collected (V'). This is shown in Figure A5.

Direct evaluation of the integral in Eq. A23 is unecessary with use of the average effluent composition, $\bar{x}_i$, since Eq. A23 can be written as,

$$x_i^o T' - \bar{x}_i\ (T' - 0) = y_i^* \tag{A24}$$

or, solving for the only unknown,

$$y_i^* = T'(x_i^o - \bar{x}_i) \tag{A25}$$

(y_i^*, x_i^o) correseponds to a point on the isotherm.

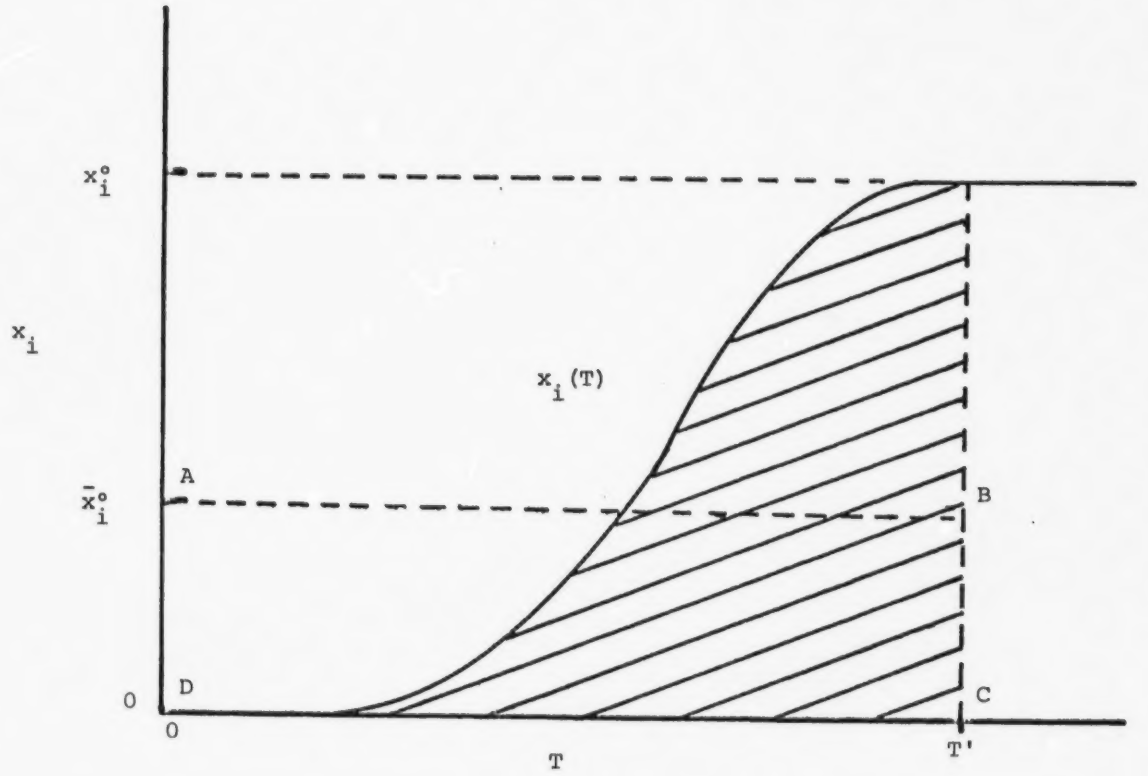

Figure A5. Column method for establishing a point on isotherm. Rectangle ABCD is equal in area to the shaded area.

3. Data

The data determined for the selenate-chloride, selenate-sulfate, selenite-sulfate and selenite-nitrate systems are listed in Table A1 through A4, respectively. For the sulfate-nitrate system, Clifford found that, for a number of strong-base anion exchangers, the average separation factor (at a total concentration of 0.005 N) was about 3.0 (35). For the chloride-bicarbonate system, see Table A5. Also, a study by Höll and Kiehling (36) found the separation factor for this system (at a total concentration of 0.01 N) to be about 3.0.

TABLE A1. SELENATE-CHLORIDE EQUILIBRIUM DATA FOR DOWEX 2X8

C_o (N)	V (ml)	m (g wet resin)	$x^*_{SeO_4}$	$y^*_{SeO_4}$
0.009817	200	7.7205	0.0221	0.0995
0.009817	200	4.7453	0.0153	0.163
0.009817	200	1.5472	0.0527	0.481
0.009817	200	3.1314	0.0323	0.252
0.09817	50	1.9706	0.455	0.453
0.09817	50	3.9367	0.246	0.376
0.0009817	400	0.2561	0.0527	0.581
0.0009817	400	0.4612	0.0350	0.329
0.0009817	400	0.6385	0.0170	0.242
0.0009817	400	1.5498	0.0050	0.101

Resin initially in chloride form ($y^o_{SeO_4} = 0$). Initial fluid-phase fraction of selenate ($x^o_{SeO_4}$) was unity.

TABLE A2. SELENATE-SULFATE EQUILIBRIUM DATA FOR DOWEX 1X8 and 2X8

C_o (N)	m (g wet resin)	$x^o_{SeO_4}$	$x^*_{SeO_4}$	$y^*_{SeO_4}$
0.009817	3.211	1.00	0.224	0.183
0.009817	1.6856	1.00	0.242	0.341
0.009817	1.1383	1.00	0.406	0.395
0.009817	0.0898	1.00	0.498	0.458
0.009817	0.4118	1.00	0.676	0.596
0.01008	3.0494	1.00	0.217	0.207
0.01008	2.5880	1.00	0.240	0.237
0.01008	1.2107	1.00	0.410	0.393
0.01008	0.8476	1.00	0.477	0.498
0.00207	3.0206	0.0098	0.00058	0.00049

Solution volume was 200 ml. Resin was initially in the sulfate form ($x^o_{SeO_4} = 0$).

TABLE A3. SELENITE-SULFATE EQUILIBRIUM DATA FOR DOWEX 1X8 AND 2X8

C_o	m (g wet resin)	$x^o_{SeO_3}$	$x^*_{SeO_3}$	$y^*_{SeO_3}$
0.10	12.05	0.10	0.065	0.0116
0.10	11.85	0.40	0.240	0.054
0.05	2.11	1.00	0.730	0.255
0.10	11.35	0.40	0.260	0.048
0.10	11.74	0.10	0.067	0.011
0.05	2.05	1.00	0.756	0.238
0.05	3.95	1.00	0.670	0.161

Solution volume was 100 ml. Resin initially in sulfate form ($y^o_{SeO_3} = 0$).

TABLE A4. SELENITE-NITRATE EQUILIBRIUM DATA FOR DOWEX 2X8

C_o	m (g wet resin)	$x^o_{SeO_3}$	$x^*_{SeO_3}$	$y^*_{SeO_3}$
0.005	0.295	1.00	0.675	0.639
0.005	0.584	1.00	0.538	0.459
0.005	1.170	1.00	0.350	0.322

Solution volume was 300 ml. Resin initially in nitrate form ($y^o_{SeO_3} = 0$).

TABLE A5. CHLORIDE-BICARBONATE EQUILIBRIUM DATA FOR DOWEX 2X8 BY THE COLUMN METHOD

Bed volume (v)	70 ml
Feed rate	0.5 ml/sec
C_o	0.083 N
Chloride feed fraction (x^o_{Cl})	0.50
Average chloride concentration in the effluent ($\bar{x}_{Cl}$)	0.323
Effluent volume (V')	5180 ml
T'	4.62
Equilibrium fraction of chloride in resin (y^*_{Cl})	0.82

APPENDIX A5

Column Experiments

The experimental data for the column runs are summarized in Tables 4 and A6. Representative effluent concentration histories are shown in Figure A6 through A9 for exhaustion runs and in Figure 12 for the regeneration run. A schematic of the experimental apparatus is shown in Figure A10.

TABLE A6. COLUMN OPERATING DATA

Run	Column Diameter (in)	Bed Height (in)	Average Flow Rate (ml/sec)	Total Solution Concentration (N)
1	0.75	10.0	0.95	0.0054
2	0.75	9.5	0.65	0.0049
3	0.75	9.8	0.55	0.0050
4	0.75	9.8	0.52	0.0050
5	0.50	15.5	0.32	0.0050
6 (Regeneration)	0.75	9.8	0.50	0.101

For all runs, Dowex 2X8 was used for which $\rho_b Q$ was 3.5 meq/g dry resin. Void fraction of beds was 0.40.

Comments on Runs 1 and 2 - In these runs, the presence of the carbonate ion lead to poor prediction of the effluent-concentration histories. Figure A6 shows a representative effluent concentration history for the major ionic constituents (sulfate, chloride, carbonate and bicarbonate) for such a run. Figure A7 shows the coresponding effluent concentration history for selenate. In each case, the ion-exchange bed was converted to the bicarbonate form by passing a 10 percent (by weight) solution of sodium bicarbonate through it. At the pH of this solution (between 8 and 8.5), there is a small fraction of carbonate present which may be taken up by the bed along with the bicarbonate ion. Predictions for this run were based on the system as a ternary system, but the presence of carbonate caused it to be a quaternary one. However, even with the disturbance due to carbonate, the breakthrough of selenate roughly coincided with the breakthrough of sulfate confirming the equilibrium prediction of the similarity of sulfate and selenate.

Comments on Runs 3 through 5 - These runs were made without bicarbonate so that the the presence of carbonate could be avoided. The aggreement between theory and experiment in these cases was quite good (see Table 4). Elimination of bicarbonate from the system served to focus attention on the behavior of selenate relative to sulfate. Figure A8 shows a representative effluent-concentration history for the major ionic components (sulfate and chloride) for such a run, while Figure A9 shows the corresponding history for selenate. Again, the breakthroughs of selenate and sulfate coincide, confirming of the similarity of sulfate and selenate.

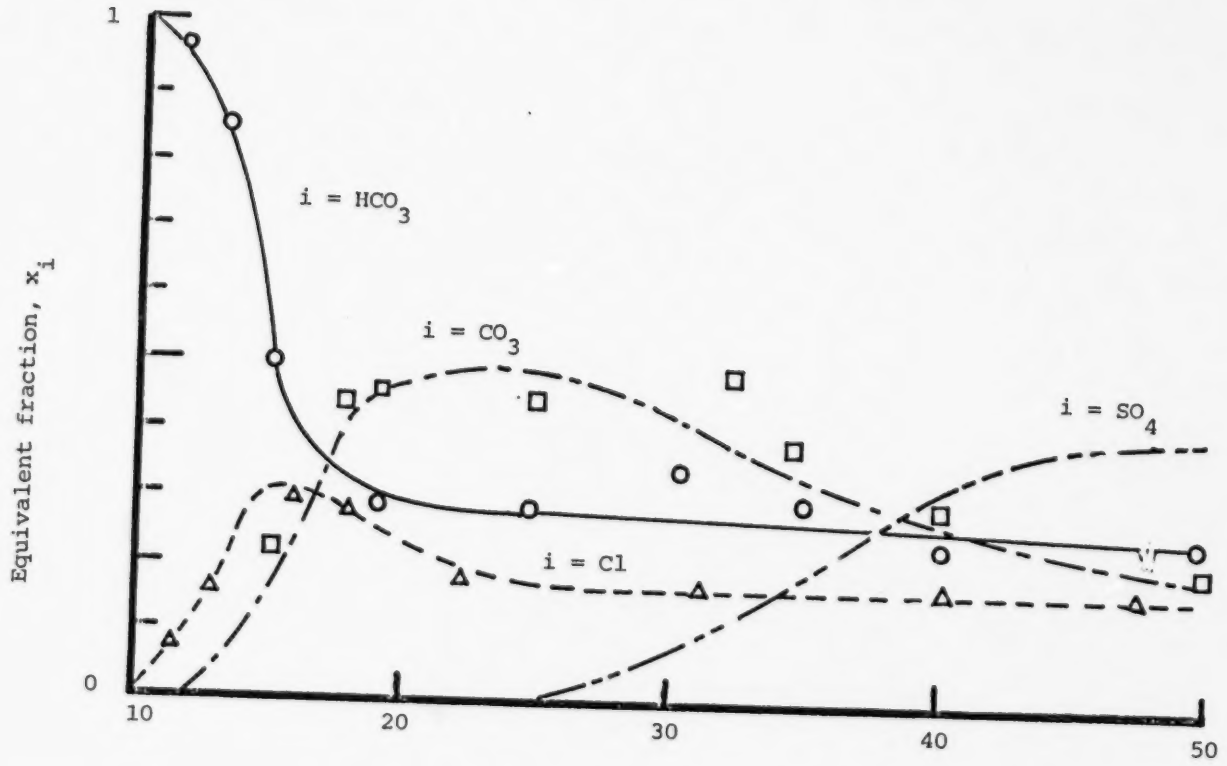

Figure A6. Effluent-concentration history for gross components in Run 2. Sulfate curve by difference.

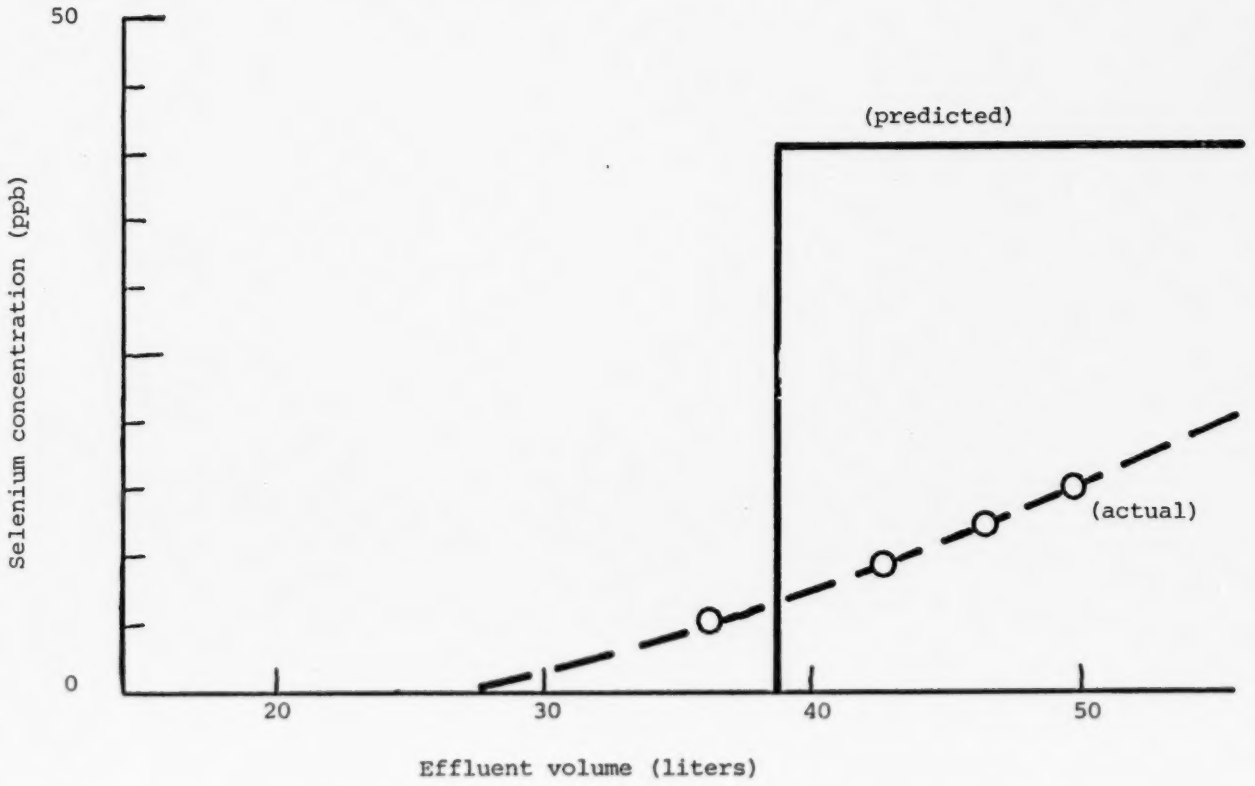

Figure A7. Effluent-concentration history for selenate in Run 2.

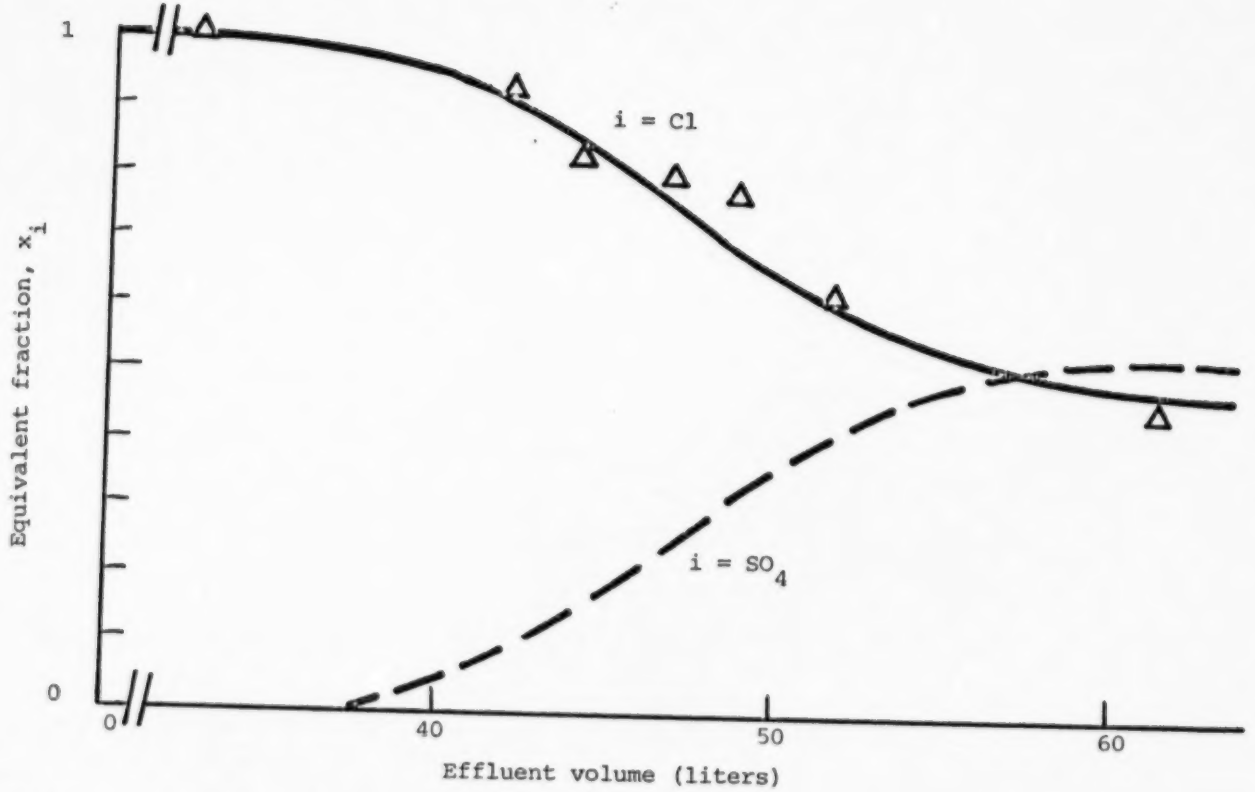

Figure A8. Effluent composition history for gross components in Run 4. Sulfate curve by difference.

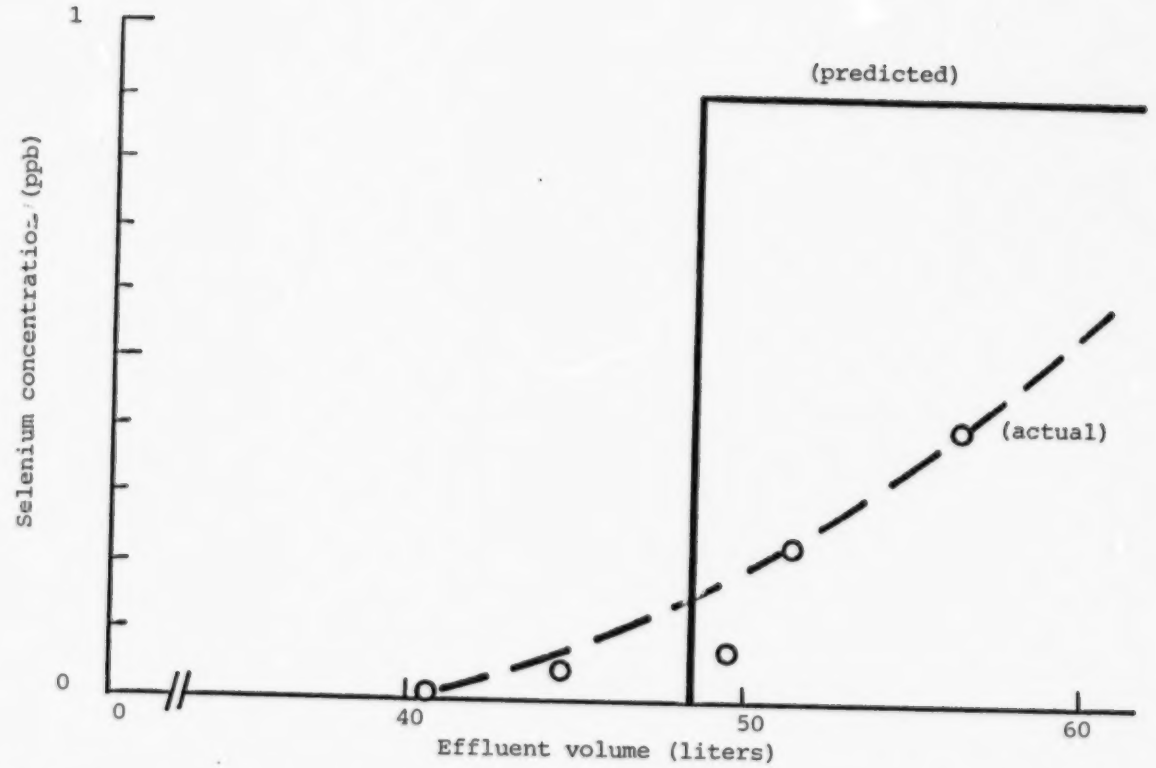

Figure A9. Effluent-concentration history for selenate in Run 4.

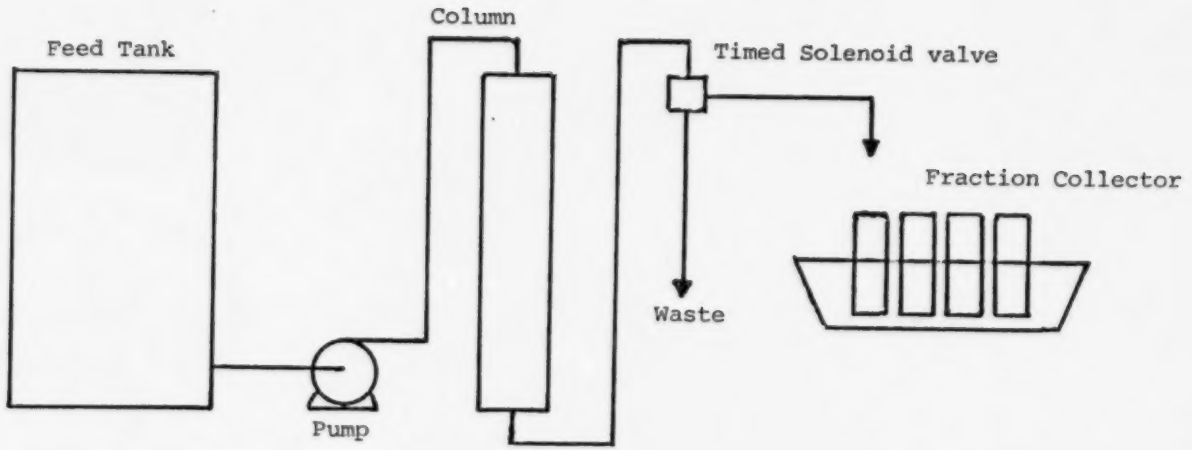

Figure A10. Experimental apparatus (schematic)

APPENDIX A6

Analytical Methods

1. Selenium:

A) Colorimetric Method (ASTM D 3081-72T, 1977 Reference 37) - This method utilized the yellow piazselenol complex formed by reaction of selenite with diaminobenzidine as the basis of a spectrophotometric determination. Selenite was the only form of selenium that could be determined and the detection range was limited to between 100 and 1000 ppb Se. The procedure proved to be time consuming.

B) Atomic Absorption Method (EPA 270.2, 1983, Reference 38) - This simple, rapid method employed flameless atomic absorption spectrophotometry to detect selenium in any form in a water sample. The procedure had a practical detection range of 20 to 150 ppb Se.

C) Catalytic Reduction Method (see References 39 and 40) - This simple method was based on the catalytic effect of selenium on the reduction of methlyene blue. It had a practical detection range of 10 to 100 ppb Se. The feasibility of this method was established, but the method was not used due to time limitations.

D) Silver Nitrate Titration - This method was developed for this study. It uses the insolubility of silver selenite, as a basis for a titration procedure similar to the chloride titration (see below). The method was limited to macroscopic concentrations of selenite (greater than about 0.01 N).

2. Sulfate:

A) Barium Precipitation Method (see Reference 41) - In this method, barium chloride, in excess, was used to precipitate sulfate. The excess barium was back-titrated with EDTA. The detection limit found in this study was about 50 ppm sulfate (using a 20 ml sample). Selenate at similar concentrations could also be determined by this method (see Table 1).

3. Chloride:

A) Silver Nitrate Titration Method (APHA Standard Methods 407 A Reference 42) - The standard method, using potassium chromate as an indicator, was reliable to around 10 ppm chloride.

4. Bicarbonate:

A) Alkalinity Titration Method (ASTM D513-80, 1981 Reference 37) - This method was used to determine the bicarbonate concentration by direct titration with a standard hydrochloric acid solution. This procedure is applicable to synthetic waters where bicarbonate is the only form of alkalinity.

(1) Mertz, W., "Essential Trace Elements", *Science*, **213**, 18 September, 1981, p. 1332.

(2) National Interim Primary Drinking Water Regulations, EPA-570/9-76-003, Office of Water Supply, Washington, DC, 1976.

(3) Weast, R. C., ed., "Handbook of Chemistry and Physics", 61st edition, CRC Press, 1981.

(4) San Francisco Chronicle, 25 November, 1983, p. 1.

(5) Sorg, T. J. and G. S. Logsdon, "Treatment Technology to Meet the Interim Primary Drinking Water Regulations for Inorganics: Part 2", *J. Amer. Water Works Assoc.*, July, 1978, p. 379.

(6) Hannah, S. A., M. Jelus and T. M. Cohen, "Removal of Uncommon Trace Metals by Physical and Chemical Processes", *J. Water Poll. Control Fed.*, November, 1977, p. 2297.

(7) Trussell, R. R., A. Trussell and P. Kreft, "Selenium Removal from Groundwater Using Activated Alumina", EPA-600/2-80-153, 1980.

(8) Sorg, T. J., R. W. Forbes and D. S. Chambers, "Removal of Radium-226 from Sarasota County, Florida, Drinking Water by Reverse Osmosis", *J. Amer. Water Works Assoc.*, April, 1980, p. 230.

(9) Linstedt, K. D., C. P. Houck and J. T. O'Connor, "Trace Element Removal in Advanced Wastewater Treatment Processes", *J. Water Poll. Control Fed.*, July, 1971, p. 1507.

(10) Wilmoth, R. C. and J. L. Kennedy, "Removal of Trace Elements from Acid Mine Drainage", EPA-600/7-79-101, 1979.

(11) Sillén, L. G. and A. E. Martell, "Stability Constants of Metal-Ion Complexes", London: The Chemical Society, 1964.

(12) Sarquis, M. and C. D. Mickey, "Selenium: Part 1 - Its Chemistry and Occurance", *J. Chem. Ed.*, **57**, 1980, p. 886.

(13) Robberecht, H. and R. Van Grieken, "Selenium in Environmental Waters: Determination, Speciation and Concentration Levels", *Talanta*, **29**, 1982, p. 823.

(14) Wheelwright, S. M., Ph.D. Thesis in Chemical Engineering, University of California, Berkeley, 1982, Chapter 5.

(15) Helfferich, F. and G. Klein, "Multicomponent Chromatography", New York: Marcel Dekker, 1970.

(16) Helfferich, F., "Ion Exchange", New York: McGraw-Hill, 1962.

(17) DeVault, D., "The Theory of Chromatography", *J. Amer. Chem. Soc.*, **65,** 1943, p. 532.

(18) Klein, G., D. Tondeur and T. Vermeulen, "Multicomponent Ion Exchange in Fixed Beds", *Ind. Eng. Chem. Fund.*, **6,** 1967, p. 339.

(19) Tondeur, D., PhD Thesis, University of Nancy, France, 1969.

(20) Rhee, H. K., R. Aris and N. R. Amundsen, "On the Theory of Multicomponent Chromatography", *Phil. Trans. Roy. Soc.*, **A267,** 1970, p. 419.

(21) Williams, R. J., "Determination of Inorganic Anions by Ion Chromatography with Ultraviolet Absorbance Detection", *Anal. Chem.*, **55,** 1983, p. 851.

(22) Hoover, T. B. and G. D. Yager, "Determination of Trace Anions in Water by Multidimensional Ion Chromatography", *Anal. Chem.*, **56,** 1984, p. 221.

(23) El-Enany, F. F., K. Mahmoud and M. M. Varma, "Microdetermination of Selenium with Ascorbic Acid", *Anal. Chem.*, **52,** 1980, p. 1540.

(24) Sinemus, H. W., M. Melcher and B. Welz, "Influence of Valence State on the Determination of Antimony, Arsenic, Bismuth, Selenium and Tellurium in Lake Constance Water Using the Hydride Atomic Absorption Technique", *Atomic Spectroscopy*, **2,** 1981, p. 81.

(25) Sant, S. B., "Kinetics of the Selenious Acid - Hydrazine Reaction", *Reaction Kinetics and Catalysis Letters*, **5,** 1976, p. 107.

(26) Williams, L. R. and P. R. Haskett, "Determination of Selenium (IV) in the Presence of Selenium (VI) Using Sulfur Dioxide", *Anal. Chem.*, **41,** 1969, p. 1138.

(27) Hughes, F. J. and D. S. Martin, "Kinetics of the Oxidation of Selenious Acid by Hydrogen Peroxide", *J. Amer. Chem. Soc.*, **59,** 1955, p. 410.

(28) Dikshitulu, L. S. A., P. Vani and V. H. Rao, "Kinetics and Mechanism of the Oxidation of Se(IV) by Ce(IV)", *J. Inorg. Nucl. Chem.*, **43,** 1981, p. 1261.

(29) Lund, W. and R. Bye, "Flame Atomic Absorption Analysis for Selenium after Electrochemical Preconcentration", *Anal. Chim. Acta*, **110,** 1979, p. 279.

(30) Gmelin's Handbuch der Anorganischen Chemie, "Selenium", Supplement B1, Berlin: Springer Verlag, 1981, p. 282.

(31) Popper, K., R. J. Bouthilet and V. Salmecka, "Ion Exchange Removal of Sodium Chloride with Calcium Chloride as a Recoverable Regenerant", *Science*, **141,** 1963, p. 1038.

(32) Page, B. W., G. Klein, F. M. Golden and T. Vermeulen, "Mixed-Bed Ion-Exchange Desalting by the Calcium Hydroxide Process", *AICHE Symp. Ser.*, No. 152, **71,** 1975, p. 121.

(33) Vermeulen, T., N. K. Hiester and G. Klein, "Adsorption and Ion Exchange", Section 16 in *Chemical Engineers' Handbook*, R. Perry and C. Chilton, eds., 5th Edition, New York: McGraw-Hill, 1973.

(34) Klein, G., M. Nassiri and J. M. Vislocky, "Multicomponent Fixed-Bed Sorption with Variable Initial and Feed Conditions. Computer Prediction of Local-Equilibrium Behavior", Paper presented at American Institute of Chemical Engineers Diamond Jubilee Meeting, Washington, DC, November, 1983.

(35) Clifford, D. and W. J. Weber, "Nitrate Removal from Water Supplies by Ion Exchange", EPA-600/2-78-052, 1978.

(36) Höll, W. and B. Kiehling, "Regeneration of Anion Exchange Resins by Calcium Carbonate and Carbon Dioxide", *Water Research*, **15,** 1981, p. 1027.

(37) American Society for Testing Materials, "Standard Methods", Part 31, *Water*, 1977.

(38) United States Environmental Protection Agency, "Methods for Chemical Analysis of Water and Wastes", EPA-600/4-79-020, Revised, March 1983.

(39) West, P. W. and T. V. Ramakrishna, "A Catalytic Method for Determining Traces of Selenium", *Anal. Chem.*, **40**, 1968, p. 966.

(40) Bowling, J. L., J. A. Dean and G. Goldstein, "Determination of Selenium in Natural Waters Using the Centrifugal Photometric Analyzer", *Anal. Lett.*, **7**, 1974, p. 205.

(41) Grether, C., "Determination of the Sulfate Ion by Poteniometric Titration", Metrohm Herisau Applications Bulletin A38e, March, 1965. Based on the results of R. Sijderius, *Anal. Chim. Acta*, **11**, 1954, p. 28. and B. N. Kabakov, *Z. Anal. Chem.*, **158**, 1957, p. 120.

(42) American Public Health Association, "Standard Methods for the Examination of Water and Wastewater", 15th edition, 1980.